Unclassified

SECURITY CLASSIFICATION OF THIS PAGE *(When Data Entered)*

REPORT DOCUMENTATION PAGE		READ INSTRUCTIONS BEFORE COMPLETING FORM
1. REPORT NUMBER TN-1771	2. GOVT ACCESSION NO. DN387307	3. RECIPIENT'S CATALOG NUMBER
4. TITLE *(and Subtitle)* A SUMMARY OF THE SEACON MOORING VALIDATION EXPERIMENT		5. TYPE OF REPORT & PERIOD COVERED Not final; Oct 1984 – Apr 1986 6. PERFORMING ORG. REPORT NUMBER
7. AUTHOR(s) Paul A. Palo, Therese McAllister, and Steve Karnoski		8. CONTRACT OR GRANT NUMBER(s)
9. PERFORMING ORGANIZATION NAME AND ADDRESS NAVAL CIVIL ENGINEERING LABORATORY Port Hueneme, California 93043-5003		10. PROGRAM ELEMENT, PROJECT, TASK AREA & WORK UNIT NUMBERS 62760N; YF60.534.091.01.A353
11. CONTROLLING OFFICE NAME AND ADDRESS Naval Facilities Engineering Command Alexandria, Virginia 22332		12. REPORT DATE June 1987 13. NUMBER OF PAGES 76
14. MONITORING AGENCY NAME & ADDRESS*(if different from Controlling Office)*		15. SECURITY CLASS. *(of this report)* Unclassified 15a. DECLASSIFICATION DOWNGRADING SCHEDULE

16. DISTRIBUTION STATEMENT *(of this Report)*

Approved for public release; distribution unlimited.

17. DISTRIBUTION STATEMENT *(of the abstract entered in Block 20, if different from Report)*

18. SUPPLEMENTARY NOTES

19. KEY WORDS *(Continue on reverse side if necessary and identify by block number)*

Moorings, current loads, cable structures, vessel moorings, vessel response, cable dynamics, hydrodynamics, ocean platform

20. ABSTRACT *(Continue on reverse side if necessary and identify by block number)*

This report presents full-scale data collected in a comprehensive mooring test of a 2,300-ldt construction barge, moored with wire rope in 50 feet of water. Wind, current, and wave excitations and all mooring system responses were measured. Measurements included static, slowly varying, and dynamic responses in slack and taut four-point moorings. Additional tests were conducted to determine single-point mooring behavior and vessel loads due

continued

DD FORM 1 JAN 73 1473 EDITION OF 1 NOV 65 IS OBSOLETE

Unclassified

SECURITY CLASSIFICATION OF THIS PAGE *(When Data Entered)*

20. Continued

to steady wind and current only. The results are summarized in the form of autospectra, probability density functions, frequency response functions, and associated uncertainty levels.

Library Card

Naval Civil Engineering Laboratory
A SUMMARY OF THE SEACON MOORING VALIDATION EXPERIMENT, by Palo, McAllister, and Karnoski
TN-1771 76 pp illus June 1987 Unclassified

1. Moorings 2. Current loads I. YF60.534.091.01.A353

This report presents full-scale data collected in a comprehensive mooring test of a 2,300-ldt construction barge, moored with wire rope in 50 feet of water. Wind, current, and wave excitations and all mooring system responses were measured. Measurements included static, slowly varying, and dynamic responses in slack and taut four-point moorings. Additional tests were conducted to determine single-point mooring behavior and vessel loads due to steady wind and current only. The results are summarized in the form of autospectra, probability density functions, frequency response functions, and associated uncertainty levels.

TN-1771
June 1987

NCEL
Technical Note

By Paul A. Palo, Therese McAllister, and Steve Karnoski

Sponsored By Naval Facilities Engineering Command

A SUMMARY OF THE SEACON MOORING VALIDATION EXPERIMENT

ABSTRACT This report presents full-scale data collected in a comprehensive mooring test of a 2,300-ldt construction barge, moored with wire rope in 50 feet of water. Wind, current, and wave excitations and all mooring system responses were measured. Measurements included static, slowly varying, and dynamic responses in slack and taut four-point moorings. Additional tests were conducted to determine single-point mooring behavior and vessel loads due to steady wind and current only. The results are summarized in the form of autospectra, probability density functions, frequency response functions, and associated uncertainty levels.

NAVAL CIVIL ENGINEERING LABORATORY, PORT HUENEME, CALIFORNIA 93043

METRIC CONVERSION FACTORS

Approximate Conversions to Metric Measures

Symbol	When You Know	Multiply by	To Find	Symbol
		LENGTH		
in	inches	*2.5	centimeters	cm
ft	feet	30	centimeters	cm
yd	yards	0.9	meters	m
mi	miles	1.6	kilometers	km
		AREA		
in^2	square inches	6.5	square centimeters	cm^2
ft^2	square feet	0.09	square meters	m^2
yd^2	square yards	0.8	square meters	m^2
mi^2	square miles	2.6	square kilometers	km^2
	acres	0.4	hectares	ha
		MASS (weight)		
oz	ounces	28	grams	g
lb	pounds	0.45	kilograms	kg
	short tons (2,000 lb)	0.9	tonnes	t
		VOLUME		
tsp	teaspoons	5	milliliters	ml
Tbsp	tablespoons	15	milliliters	ml
fl oz	fluid ounces	30	milliliters	ml
c	cups	0.24	liters	l
pt	pints	0.47	liters	l
qt	quarts	0.95	liters	l
gal	gallons	3.8	liters	l
ft^3	cubic feet	0.03	cubic meters	m^3
yd^3	cubic yards	0.76	cubic meters	m^3
		TEMPERATURE (exact)		
°F	Fahrenheit temperature	5/9 (after subtracting 32)	Celsius temperature	°C

*1 in = 2.54 (exactly). For other exact conversions and more detailed tables, see NBS Misc. Publ. 286, Units of Weights and Measures, Price $2.25, SD Catalog No. C13.10:286.

Approximate Conversions from Metric Measures

Symbol	When You Know	Multiply by	To Find	Symbol
		LENGTH		
mm	millimeters	0.04	inches	in
cm	centimeters	0.4	inches	in
m	meters	3.3	feet	ft
m	meters	1.1	yards	yd
km	kilometers	0.6	miles	mi
		AREA		
cm^2	square centimeters	0.16	square inches	in^2
m^2	square meters	1.2	square yards	yd^2
km^2	square kilometers	0.4	square miles	mi^2
ha	hectares (10,000 m^2)	2.5	acres	
		MASS (weight)		
g	grams	0.035	ounces	oz
kg	kilograms	2.2	pounds	lb
t	tonnes (1,000 kg)	1.1	short tons	
		VOLUME		
ml	milliliters	0.03	fluid ounces	fl oz
l	liters	2.1	pints	pt
l	liters	1.06	quarts	qt
l	liters	0.26	gallons	gal
m^3	cubic meters	35	cubic feet	ft^3
m^3	cubic meters	1.3	cubic yards	yd^3
		TEMPERATURE (exact)		
°C	Celsius temperature	9/5 (then add 32)	Fahrenheit temperature	°F

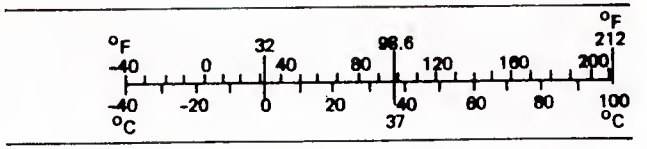

CONTENTS

INTRODUCTION

SEADYN/DSSM is a general-purpose mooring model capable of simulating the responses of complex, arbitrarily configured systems (Ref 1). This model was developed at the Naval Civil Engineering Laboratory (NCEL), under sponsorship of the Naval Facilities Engineering Command (NAVFAC), Work Unit YF60.534.091.01.A353. Essentially, it is an integrated collection of mathematical models. These models include cable responses, vessel motion, vessel wind loads, vessel current loads, vessel drift loads, and system equations of motion. Each of these models has an accuracy and applicability determined by various assumptions and simplifications (Ref 2), such as linearity, stationarity, and decoupling. While each model can be individually validated, the validity of the assembled models cannot be established until computed results are compared to reliable measurements of actual system behavior.

SEADYN/DSSM has an inherent weakness shared with most simulation models--many problem inputs cannot be accurately specified because of the lack of reliable information. Examples include vessel drag force and yaw moment coefficients associated with wind, current, and wave groups (drift forces). Errors and simplifications in the calculation procedure as well as errors in the environmental measurements cause differences between the simulated and measured responses, even if the computer model is correct. Care must be taken in any validation to differentiate between measurement errors and incorrect model behavior.

Accordingly, a Mooring Validation Experiment (MVE), sponsored by NAVFAC, was conducted to provide reliable measurements of the total mooring system behavior and environmental conditions. These data were then used to validate specific parts of SEADYN/DSSM (vessel loads, static offset, vessel dynamics, etc.) and to simulate the assembled system response (e.g., equilibrium position, dynamic line tensions). The various tests and their objectives are listed in Table 1.

The purpose of this report is to describe the mooring configurations and test measurements. Some data reductions, such as autospectra and probability density functions, are also included to supplement the data and demonstrate its quality. Interpretation of this basic information will be included in a followup report of the SEADYN/DSSM validation results.

TEST VESSEL

The test vessel was NAVFAC's offshore construction platform (OCP) SEACON, a converted YFNB barge. The dimensions of the SEACON are as follows:

Overall Length	260 ft
Moulded Beam	48 ft
Displacement	
Light	831 ldt
Fully Loaded	2,780 ldt
For MVE Tests	2,340 ldt
Draft	
Light	3 ft 6 in
Fully Loaded	9 ft 6 in
For MVE Tests	8 ft 6 in
Hull Depth	15 ft 1 in
Superstructure Height Above Main Deck	30 ft
Longitudinal Center of Buoyancy	
From Forward Perpendicular	129.1 ft
From Midship	0.9 ft
Longitudinal Center of Flotation	
From Forward Perpendicular	135.8 ft
From Midship	-5.8 ft
Vertical Center of Buoyancy	
Above Midship	4.4 ft
Transverse Moment Above Baseline	28.5 ft
Wind Areas for Test Draft	
Head Wind Area	1,512 ft^2
Beam Wind Area	
Hull	1,690 ft^2
Superstructure	2,250 ft^2
Natural Roll Period	6 s

Figure 1 presents specific information on this vessel.

The SEACON was chosen for two reasons. First, measurements of its seakeeping characteristics would be directly usable by its operators in future projects. Second, the SEACON has two features that were used to full advantage in this test: cycloidal propulsion, which allowed for thrust in all directions (this was used in the static watchcircle test); and a self-contained four-point mooring capability, which minimized mooring installation and recovery costs.

TEST SITES

The primary test site was 3 km east of Duck, North Carolina, in 55 feet of water. Figure 2 shows this site (taken from Ref 3), which was chosen because of the environmental support available from the Field Research Facility (FRF), which is supported by the U.S. Army Corps of Engineers Waterways Experiment Station. This offshore site allowed for true open-ocean environmental excitation, with some wave shoaling effects due to the shallow (55-foot) water depth.

The wind and current loads test was conducted at a second test site within Chesapeake Bay at Whiskey Anchorage, shown in Figure 3 (taken from Ref 4). This site was chosen because it offered a sheltered site (no waves) with moderate (1-knot) currents. Thus, mooring loads at this site were due to steady wind and current loads only.

INSTRUMENTATION

Data were collected in a variety of locations including onboard the SEACON, in the water column, and onshore at the FRF. These sites are individually described below.

A small minicomputer (DEC 11/03) was used to control the data acquisition process and store data onboard the SEACON. This computer collected the following information every half second: cable tension, vertical angle, and compass heading for all four lines; vessel accelerations, displacements, and rotations; wind speed and direction; and wave amplitudes and direction. Filtering was not used.

The vessel motions were measured by an unstabilized, five-degree-of-freedom (no yaw) motion sensing package from Systron-Donner, Inc., Concord, CA. This package was located at midship, centered on the deck. No significant contamination of the measurements is expected because the package placement was near the vessel center of rotation (which eliminates angular effects in the translational measurements) and because the vessel motions were small (Euler angles not required).

SEACON position measurements were taken using an onboard Mini-Ranger system. These measurements provided information on the anchor placement and recovery positions and on the mean and slowly varying displacements of the SEACON during the various tests. These latter low-frequency/low-acceleration measurements were taken every 15 seconds and later combined with the Systron-Donner measurements to get the total SEACON motions. The Mini-Ranger measurements were taken relative to a true north-east axis system, rounded off to whole meters. These data were converted to an NCEL system of true south-east represented by X and Y, respectively, with an origin at an approximate equilibrium vessel position for the four-point mooring.

The U.S. Army Waterways Experiment Station's Field Research Facility (FRF) helped NCEL collect wave, wind, and current data at Duck, NC. A summary of these data is presented in Reference 5.

Two Waverider buoys were used to measure wave amplitudes and direction in close proximity to the ship. Their location relative to the vessel and the data collected is described in Appendix A.

The FRF measurements included wind speed and wave and their directions. Wave amplitude was recorded from the two Waverider buoys by the SEACON, from a Baylor wave staff mounted at the end of the FRF pier

(1,800 feet from shore in a water depth of 25 feet), and a third Waverider buoy north of the ship. Wave direction was determined from a radar-based instrument that shows wave scatter. A wind anemometer mounted on the FRF building provided a secondary source of wind data.

Three self-recording Neil Brown acoustic vector measurement current meters were used in an array around the SEACON as shown in Figure 2. The two nearshore meters were located at depths of 14.5 and 29 feet below mean sea level. Measurements of current direction from the farshore meter at 14.5 feet could not be used because the factory used an incorrect circuit card that made the directional data invalid, so only the nearshore measurements are presented.

TEST SCHEDULE

The tests were scheduled to take advantage of the different environmental excitation levels that occurred over the 4-day test period. Table 2 summarizes the tests and environment for each test day. Tests 3 and 5 are supporting tests. Test 3 will be used to confirm the static four-point mooring configuration and stiffness. Test 5 will provide information on the steady wind-induced and current-induced loads on the SEACON. Data from these tests will be used to validate the static simulation capability of SEADYN, which must be known before the dynamic simulations can be made. Appendix B summarizes the environmental data for the test period.

DATA ANALYSIS

A number of analyses were performed to isolate the static and dynamic characteristics of the mooring responses. The particular analysis chosen for each test and the associated results are discussed in subsequent sections. A description of each analysis technique is contained here.

A time domain analysis includes statistical and probabilistic analyses. The statistical analyses determined the mean; mean (linear) slope; root-mean-square (rms); and maximum values for tension, displacement, and other parameters. The probability density function for selected data channels was calculated and is presented against the corresponding normal distribution for each sample interval. A graphical display of sampled data versus time is provided to allow for subjective analysis of the data quality and parameter behavior.

Frequency domain analyses were conducted using standard spectral analysis techniques as outlined in Reference 6 (and others). This information includes one-sided autospectra, frequency response functions, coherence, and phase as functions of frequency (cycles/s). The following parameters were used:

Sampling period = 0.5 s
No. of samples per subrecord = 1,024
No. of subrecords per test = 4

From these,

Frequency resolution = 0.002 Hz
Nyquist frequency = 1 Hz
Subrecord length = 512 s

The results of the frequency analysis are presented on graphs using integer frequency bandwidth increments.

Three types of analyses were conducted for the four-point tests to identify different mooring phenomena. The first analysis investigated the characteristics of an individual channel, such as its mean value, rms value, and normality. The second analysis investigated the relationship between two directly measured channels, such as wave amplitude and vessel heave. The third analysis investigated the relationship between two derived (calculated) records, such as the wave envelope and net mooring forces. In some cases the analysis is self-explanatory. The significance and limitations of each analysis are discussed in the subsequent sections.

Four-Point Mooring Dynamics Tests

The four-point mooring configuration with anchor position and line length information is presented in Figure 4. The mooring measurements were taken in eight separate tests between 1140 and 1740 on 15 November. These are further separated into four "slack" tests and, after two of the line lengths were shortened, four "taut" tests. Each test lasted about one-half hour. The tests measurements are summarized in Table 3.

The excitations were sufficient to induce all the mooring phenomena under study but not large enough to challenge the limits of the models. The wind stayed relatively constant at 17 knots and rotated from southeast to south-southwest during these tests. The current was small and from the north. The waves contained three wave trains--a small swell incident from the northeast (only for slack tests); fully developed ocean waves that were initially beam-on from the east; and local, fetch-limited storm chop initially from the east-southeast (see Figure 4). The latter two wave angles rotated continuously throughout the four-point tests to a final wave direction from the southeast.

The slack moorings were excited by long-period beam waves and shorter period quartering waves, while the taut moorings had long quartering and shorter almost stern-on waves. This provided an excellent range of excitation frequencies and incident angles for validation of the vessel motion models.

Appendix C presents sample test measurements and analyses for the four-point test series. The current measurements are in Appendix B.

Some observations regarding these tests are:

1. The significant wave height for all tests was between 5 and 6 feet, with fairly equal proportions of energy between the open-ocean waves and storm chop in each test. The open-ocean modal period was constant at 10 seconds, while the storm-wave modal period increased from 4 to 5.4 seconds between the first and last tests. The incident direction of both wave trains rotated during the tests. The wave spectra are shown in Appendix C.

2. The vessel angular response stayed constant throughout the tests, with a mean heading of 343 degree-true and a rms yaw amplitude of 8°

3. The first-order vessel translations had average significant amplitudes of 0.5 foot for surge, 1.0 foot for sway, and 1.0 foot for heave. Average significant angular amplitudes were 0.4° for pitch, 1.6° for roll, and 7.7° for yaw. (The yaw measurements were made from time series recordings of vessel heading.)

4. The closest wave buoy was positioned 260 feet (five water depths) away from the SEACON and approximately aligned in the direction of the incident wind waves. This separation distance was chosen to avoid data contamination from waves reflected by the vessel. The wave time series data measured at each buoy were of excellent quality, having little or no noise or equipment contamination. The autospectra for each buoy is, therefore, also of excellent quality. Appendix A contains additional information on the wave buoy data.

5. Line tensions ranged from 0 (slack) to about 75,000 pounds (maximum). Tensions were not normally (Gaussian) distributed (see Figure 5).

6. The amplitude of the slowly varying watchcircle was 20 feet for the slack tests and 15 feet for taut tests.

Static Watchcircle Tests

A series of tests was conducted to measure the static watchcircle of the four-point mooring with no wave effects (i.e., slow drift or dynamic). The SEACON's propulsion units were used to add thrust at various levels of power and orientation, and the net mooring forces and vessel displacement were calculated. About 10 minutes were allowed for the mooring to come to equilibrium after the vessel thrusters were applied. This information was used to determine the engine thruster forces, to verify the measured anchor positions shown in Figure 4a, and to validate the SEADYN/DSSM static equilibrium calculations.

The entire series of tests lasted 2 hours. The environmental loads were fairly constant during this period. Small currents of 0.1 knot came from the northwest, 20-knot winds came from the west to southwest directions, and small waves came from the west (2-foot significant wave height). The currents were measured about 15 feet below the surface to avoid wave contamination (see Table 2); no data were obtained on the surface currents.

Test results for the engine thrust levels are summarized in Table 4 and plotted in Figure 6. The first test had no thrusters applied so that the environmental forces could be measured. The forces from this first reference test were then subtracted from the total mooring forces measured in the other tests to determine the forces exerted by the engine thrusters. The thruster forces are tabulated in Table 4 under the "Calculated Thrust" column. Analysis of the data indicates that the average 50-percent and 100-percent thrust values are 5,600 and 11,000 pounds, respectively. As shown in Figure 6, the total resultant

thrust is essentially twice as large in the longitudinal directions compared to the lateral direction. The insert in Figure 6 shows the position of the thrusters on the SEACON. The directional dependency is considered due to wake interference effects of the stern thrusters.

The anchors did drag throughout the test period as evidenced by both the Mini-Ranger coordinates of installation and retrieval, and by the Mini-Ranger coordinates of the vessel during the various tests and the known line lengths. All of this is shown in Figure 4a.

The most direct evidence of anchor drag is seen in the disparity between the installed and retrieved coordinates for each leg, as shown in Figure 4b.

Figures 4c and 4d illustrate the indirect method for establishing the anchor coordinates for each test. For this check, the vessel chock positions are established from a given vessel position (from the Mini-Ranger data) and the vessel heading (from compass readings). Then, the known horizontal line projections (radii) are added, which results in a locus of possible points for the anchor. By assuming that the anchor dragged in a straight line between the installed and retrieved positions, an estimate of the anchor position can be made for each test. Figure 4c shows this process for the 4-point dynamic test while Figure 4d shows a reconstruction from the static watchcircle tests (note the difference in the arcs for both stern lines between Figures 4c and 4d. The lack of consistency in the bow port anchor coordinates could not be resolved better than that shown in the figures.)

Single-Point Mooring (SPM) Tests

These tests were conducted with negligible waves, small current, and a strong steady wind. These quasi-steady excitations produced large, oscillating lateral vessel excursions (fishtailing) because of the strong wind-induced yaw moment caused by the forward location of the superstructure.

The SPM test configuration is shown in Figure 7. Representative time series plots of vessel heave, wind angle, vessel heading, and hawser tension are shown in Figures 8 through 11. Figure 11 shows the vessel heave, which was small, typically less than 0.5 foot. Wave grouping can be seen in this figure, but this secondary force is negligible due to the small wave height relative to the vessel size. The wind was the predominant exciting force. The wind speed ranged between 15 and 20 knots. The local wind angle variation (relative to the ship centerline) is shown in Figure 9. Over the duration of these figures (9 minutes), the local wind angle varied between 300° and 40°. Figure 8 is a time series plot of the variation in the vessel heading, which is illustrated in Figure 7. (Note the direct correlation between the wind angle variation and the corresponding vessel heading.) Figure 10 shows the hawser tensions that occurred while the vessel oscillated from side to side. The first tension spike occurs when the bow lateral displacement is stopped by the hawser. The vessel center of gravity continues to rotate about the bow, until it overshoots the relative wind angle which reverses the vessel rotation. The oblique vessel/wind angle due to this overshoot presumably results in additional longitudinal and lateral drag causing the second tension spike. The

tension remains fairly constant as the vessel swings to the other side. Another tension spike is seen in Figure 10 as the vessel repeats the cycle just described.

Steady Wind and Current Load Tests

The objective of these tests was to collect data to allow for evaluation of the SEACON wind and current loads. With this information, SEACON mean and slowly-varying drift forces could be estimated by subtracting these wind and current forces and yaw moments from the total mooring forces in the four-point tests.

Analyses of current-induced loads from recent tests (Ref 7) clearly show the sensitivity of the lateral force coefficient to the vertical current shear. Unfortunately, the shear was not measured in the MVE tests. This limits the usefulness of these tests and requires additional analyses to deduce qualitative information.

The data and analyses for these tests are included in Table 5 and Figures 12 and 13. The lack of surface current measurements was alleviated with the following procedure:

1. Assume that the lateral current force coefficient is some unknown (monotonic) function of the vertical shear.

2. Assume a magnitude for the surface current, which defines the vertical shear when combined with the measured current at 15 feet; iterate for coefficient-shear pairs for each test so that the overall function is continuous; this relationship calculated for these tests is shown in Figure 13.

3. Examine the chronological behavior of the resulting (calculated) surface current velocity and vertical shear for continuity; refer to the respective columns in Table 5.

Conclusions from this analysis are:

1. Chronological examination of the current field shows good continuity, establishing that this procedure was valid. Note that large variations in the shear are expected as the tide reverses in the steady wind field.

2. Results are considered constant since Reynolds Number (based on twice the draft) varied from 1.3 to 2.3 x 10^6.

3. The results in Figure 12 are considered excellent in a qualitative sense and clearly show: the linear relationship between lateral drag coefficient (C_Y) and normalized vertical shear (NVS), the limits of that linearity, the symmetrical nature of the relationship for positive and negative shears, and the same coefficient value for uniform flow conditions as was found in the results presented in Reference 7.

4. The linear slope found here differs from that found in Reference 7. However, that could easily be a consequence of the different definitions (depth of measurement compared to vessel draft) of NVS between the reports.

5. The magnitudes of the vertical shears inferred in these calculations are comparable to the shears reported in Reference 7. The applicability of the latter results to usual mooring design problems had been questioned because of concerns that the topography at that test site might have amplified the shear. Since the magnitudes of these shears are therefore considered representative, then the variation in the coefficients is likewise considered as an important parameter for design purposes.

SUMMARY

The general quality of data collected during the Mooring Validation Experiment was good. Sufficient environmental conditions existed to cause significant loads and displacements in the various mooring configurations. The environmental and mooring data, presented in this report, were found to be consistent and in keeping with expected values.

Of the four test series conducted, all are suitable for SEADYN/DSSM validation purposes except for the single-point mooring tests (which were nonstationary). In those tests the system did not reach a steady equilibrium position; the data are therefore not suitable for the small-displacement frequency domain dynamics used in the SEADYN/DSSM analysis. The rest of the MVE data will be used to determine the validity of the solutions given by the frequency domain analysis method for vessel dynamics.

The SEACON's thruster forces and seakeeping characteristics were directly measured during these tests. The vessel's thrusters had an average 50-percent thrust of 5,600 pounds and 100-percent thrust of 11,000 pounds, with the longitudinal thrust about twice as large as the lateral thrust. The vessel's natural roll period was measured to be 6 seconds.

The trend observed in the steady current test data was found to qualitatively agree with the trend found in similar full-scale tests reported in Reference 7. In both cases the lateral drag coefficient is a function of the vertical current shear.

REFERENCES

1. P.A. Palo, D.J. Meggitt, and W.J. Nordell. "Dynamic cable analysis models," Offshore Technology Conference, Houston, Tex., May 1983. (OTC 4500)

2. P.A. Palo. "Development of a general-purpose mooring analysis capability for the U.S. Navy," paper presented at the Society of Naval Architects and Marine Engineers, San Diego Section, 20 Feb 1985.

3. U.S. Department of Commerce, National Oceanic and Atmospheric Administration. National Ocean Survey, Chart 12204: Currituck Beach Light to Wimble Shoals, 26th edition. Washington, D.C., 21 Feb 1981.

4. _____. National Ocean Survey, Chart 12245: Hampton Roads, 46th edition. Washington, D.C., 30 Jul 1983.

5. U.S. Army Corp of Engineers, Waterways Experiment Station, Coastal Engineering Research Center. Final Report: Oceanographic and meteorological conditions during a ship mooring force study, by C. Mason, W.E. Grogg, Jr., and E.W. Bichner. Vicksburg, Miss., Dec 1984.

6. J.S. Bendat and A.G. Piersol. Random data: Analysis and measurement procedures. New York, N.Y., John Wiley & Sons, Inc., 1971.

7. _____. Technical Note N-1749: Current-induced vessel forces and yaw moments from full-scale measurements, by P.A. Palo. Port Hueneme, Calif., Mar 1986.

8. P.A. Palo. "Steady wind- and current-induced loads on moored vessels," Offshore Technology Conference, Houston, Tex., May 1983. (OTC 4530)

9. U.S. Army Corp of Engineers, Waterways Experiment Station, Coastal Engineering Research Center. Miscellaneous Paper CERC 84-7: Spatial variability in the nearshore wavefield, by S.A. Hughes. Vicksburg, Miss., Jul 1984.

Table 1. MVE Tests and Objectives

Test	Objective
Static Watchcircle	- Confirm anchor placement measurements - Validate SEADYN/DSSM static equilibrium calculations - Measure SEACON engine thrust vectors
Four-Point Mooring	- Measure system responses in slack mooring - Measure system responses in taut mooring
Single-Point Mooring (SPM)	- Determine vessel characteristic SPM behavior (e.g., stability)
Wind and Current	- Isolate wind and current loads - Use in four-point mooring analysis to isolate drift forces

Table 2. Test Schedule and Average Environmental Conditions

Test[a]	Date	Test	Wind Speed (ft/s)	Significant Wave Height (ft)	Current Speed (ft/s)
1	15 Nov 1984	Slack four-point	29	5.0	1.6
2	15 Nov 1984	Taut four-point	26	5.5	0.6-1.6
3	16 Nov 1984	Static watchcircle	16-33	0-3.3	0.1-0.6
4	17 Nov 1984	Single-point mooring	33	1.0	0.6
5[b]	18-19 Nov 1984	Chesapeake Bay wind and current	10-25	0	0-3.2

[a]All tests were conducted off Duck, NC, except for test 5.

[b]Currents in test 5 are due to tidal flows.

Table 3. Summary of MVE Four-Point Mooring Data

Parameter	Slack Mooring Test Number				Taut Mooring Test Number			
	1	2	3	4	5	6	7	8
Time, min	31	35	35	21	34	30	33	31
Maximum Wave Height, ft	7.9	9.4	9.3	8.8	9.6	9.6	10.5	9.3
Significant Wave Height, ft	4.6	4.9	5.1	5.2	5.2	5.5	6.0	5.4
Mean Wind Speed, kn	17.5	16.5	16.8	18.2	15.8	16.5	15.8	14.8
Steady Port Bow Line Tension, lb -mean	630	540	490	400	9,120	8,400	8,400	7,900
-rms	710	630	570	570	11,100	10,400	---[a]	9,700
-maximum	1,180	1,580	930	930	18,300	18,600	19,400	26,400
Drift Forces Starboard Bow Line Tension, lb -mean	17,200	16,100	10,100	9,300	6,000	5,700	6,000	4,500
-rms	23,000	22,800	15,400	14,300	---	---	---	6,700
-maximum	41,100	44,900	35,700	35,900	23,200	20,100	38,900	19,000
Port Stern Line Tension, lb -mean	0	0	0	0	6,300	5,000	5,000	5,300
-rms	0	0	0	0	12,300	9,600	---	10,300
-max	40	1,990	1,900	1,500	39,000	30,300	37,700	39,200
Starboard Stern Line Tension, lb -mean	24,300	23,200	16,100	15,500	13,300	14,200	14,800	11,300
-rms	35,700	35,900	27,500	26,600	23,100	---	---	19,300
-maximum	67,800	73,300	73,500	70,500	65,530	66,500	70,400	48,200
Roll Amplitude, ±deg -rms	1.5	1.5	2.2	1.6	---	---	---	1.8
-maximum	5.1	6.3	7.2[b]	5.5	6.8	6.3	6.6	6.0

Table 3. Continued

Parameter	Slack Mooring Test Number				Taut Mooring Test Number			
	1	2	3	4	5	6	7	8
Pitch Amplitude, ±deg								
-rms	0.6	0.2	1.0[b]	0.6	0.2	---	---	0.3
-maximum	1.5	1.5	5.6[b]	1.5	1.5	1.6	1.7	1.5
Yaw Amplitude, ±deg								
-mean heading	336	335	336	336	336	336	336	337
-rms	7.7	7.7	7.6	7.9	7.4	7.6	---	7.6
-maximum	22.5	24.0	25.5	27.0	27.0	25.0	12.3	25.0
Surge Amplitude, ±ft								
-rms	0.4	0.5	4.4[b]	0.5	0.5	0.6	---	0.5
-maximum	1.5	1.9	14.5[b]	2.3	1.8	1.9	1.9	1.8
Sway Amplitude, ±ft								
-rms	0.8	1.1	1.9	1.0	0.9	1.1	---	0.8
-maximum	2.5	3.1	3.2	3.0	3.2	3.6	3.2	2.9
Heave Amplitude, ±ft								
-rms	0.8	0.9	1.2	1.8	0.9	0.9	---	0.8
-maximum	2.5	2.7	3.1	3.0	3.1	3.0	2.9	2.7

[a] No values available.

[b] Values were recorded but are suspect.

Table 4. MVE Static Watchcircle Data

Test[a]	Indicated[b]		Calculated[c]	
	% Total Thrust	Indicated Thrust Angle (°)	Thrust Angle (°)	Thrust (lb)
1	0	0	0	0
2	50	0	10	6,300
3	50	60	65	4,000
4	50	90	121	4,400
5	50	120	155	5,800
6	50	180	184	7,700
7	100	180	182	16,800
8	100	120	114	7,400
9	100	90	96	8,700
10[d]	100	60	82	9,700

[a]30 min was allowed for each test configuration to reach equilibrium.

[b]Thrust vector relative to the bow as indicated by vessel equipment during the test.

[c]Calculated from the measured hawser tension vectors.

[d]Line parted after this test while moving to next position.

Average of 50% thrust measurements: 5,600 lb.

Average of 100% thrust measurements: 11,000 lb.

Table 5. Wind and Current Test Data and Analysis

Test	Vessel Heading (°)	Mooring Configuration					Wind		Current		Calculations				
		Hawser Tensions (lb)		Local Hawser Heading[a] (°)		Lateral Mooring Force[b] (lb)	Velocity (ft/s)	Local Incident Direction[a] (°)	Velocity (14.5 ft) (ft/s)	Local Incident Direction[a] (°)	Lateral Wind Force[c] (lb)	Lateral Current Force (lb)	Coefficient-Shear Values		
		Bow	Stern	Bow	Stern								C_y	NVS	$\bar{V}^f$ (ft/s)
2	337	4,650	5,680	-10	-35	-4,060	9	110	0.2	-105	460	3,600	1.6	0.80	1.00
3	336	5,500	6,850	-10	-45	-5,790	10	110	0.23	-105	560	5,230	1.6	0.80	1.2
4	330	3,650	6,030	-25	-60	-6,760	8	85	1.15	-95	380	6,380	1.2	0.25	1.55
5	330	3,900	6,390	-30	-55	-7,180	2	100	1.54	-95	10	7,170	1.1	0.10	1.70
7	327	2,590	4,180	-40	-70	-5,595	19	80	2.36	-90	2,060	3,535	0.6	-0.45	1.65
8	327	1,570	2,930	-40	-70	-3,760	15	75	2.62	-90	1,280	2,480	0.45	-0.65	1.60
9	331	1,070	1,900	-40	-60	-2,335	16	80	2.46	-95	1,460	880	0.30	-1.15	1.15
12	336	3,400	3,660	30	5	2,020	16	125	0.46	70	1,330	-3,350	1.3	0.60	1.10
13	338	430	1,230	35	25	765	23	140	1.74	70	2,120	-2,890	0.7	-0.25	1.35
16	356	920	4,370	-55	-65	-4,710	16	165	1.31	-130	200	4,510	1.0	0.10	1.40
17	0	1,455	5,310	-60	-60	-5,860	25	165	1.80	-135	720	5,140	0.8	-0.05	1.70
18	0	1,450	4,300	-60	-60	-4,975	24	140	2.30	-135	2,320	2,655	0.5	-0.50	1.55
19	4	900	2,500	-60	-60	-2,945	24	175	3.22	-140	480	2,465	0.35	-0.80	1.80

[a]Local angles measured clockwise from ship centerline; accurate to ±5°.

[b]Lateral force positive to starboard.

[c]Based on methodology in Reference 8, with a 0.8 scale factor as recommended in Reference 7.

[d]Lateral current force coefficient, including angle dependence.

[e]NVS = normalized vertical shear = $[\bar{V}-V(15)]/\bar{V}$.

[f]Calculated current speed at middraft corresponding to the C_y-NVS pair.

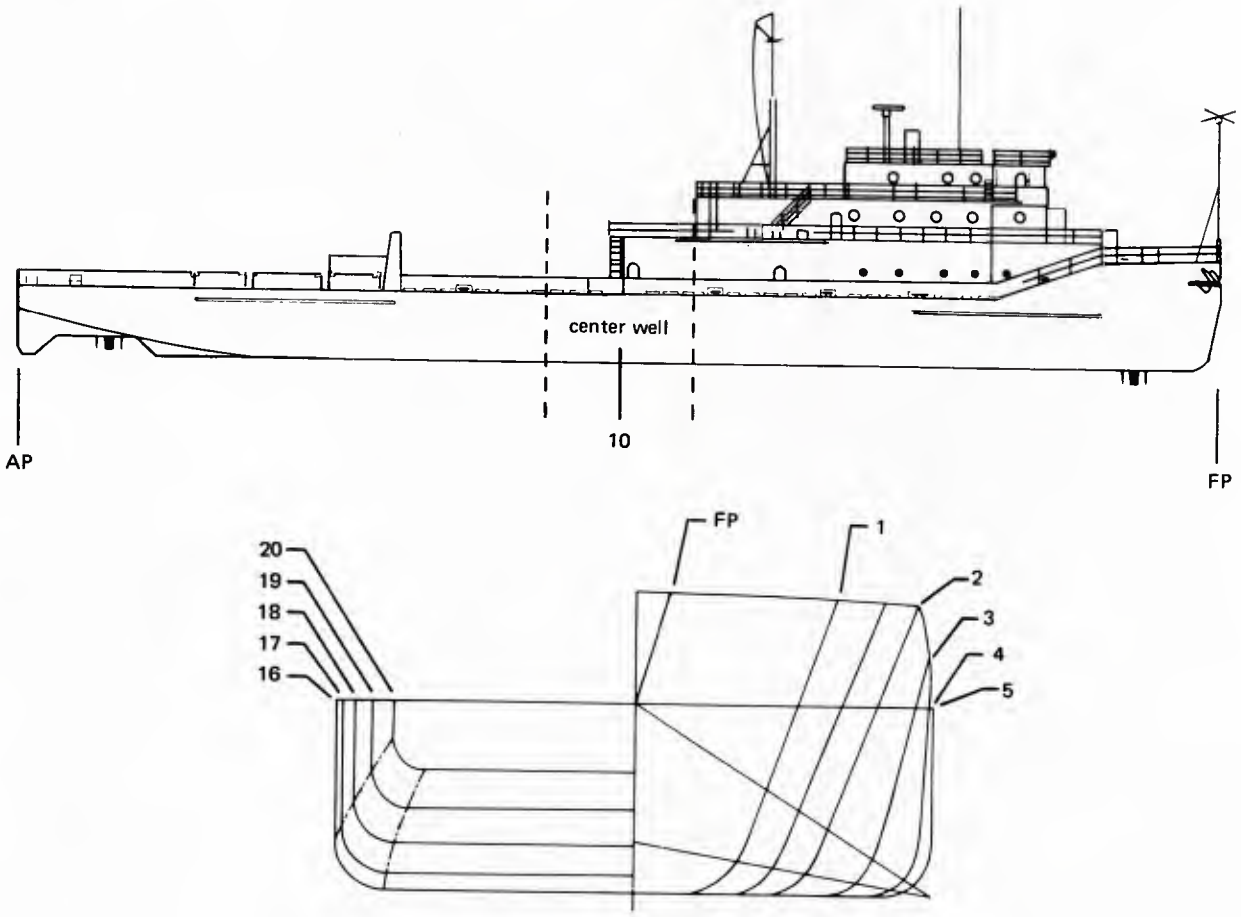

Figure 1. SEACON profile and lines drawing.

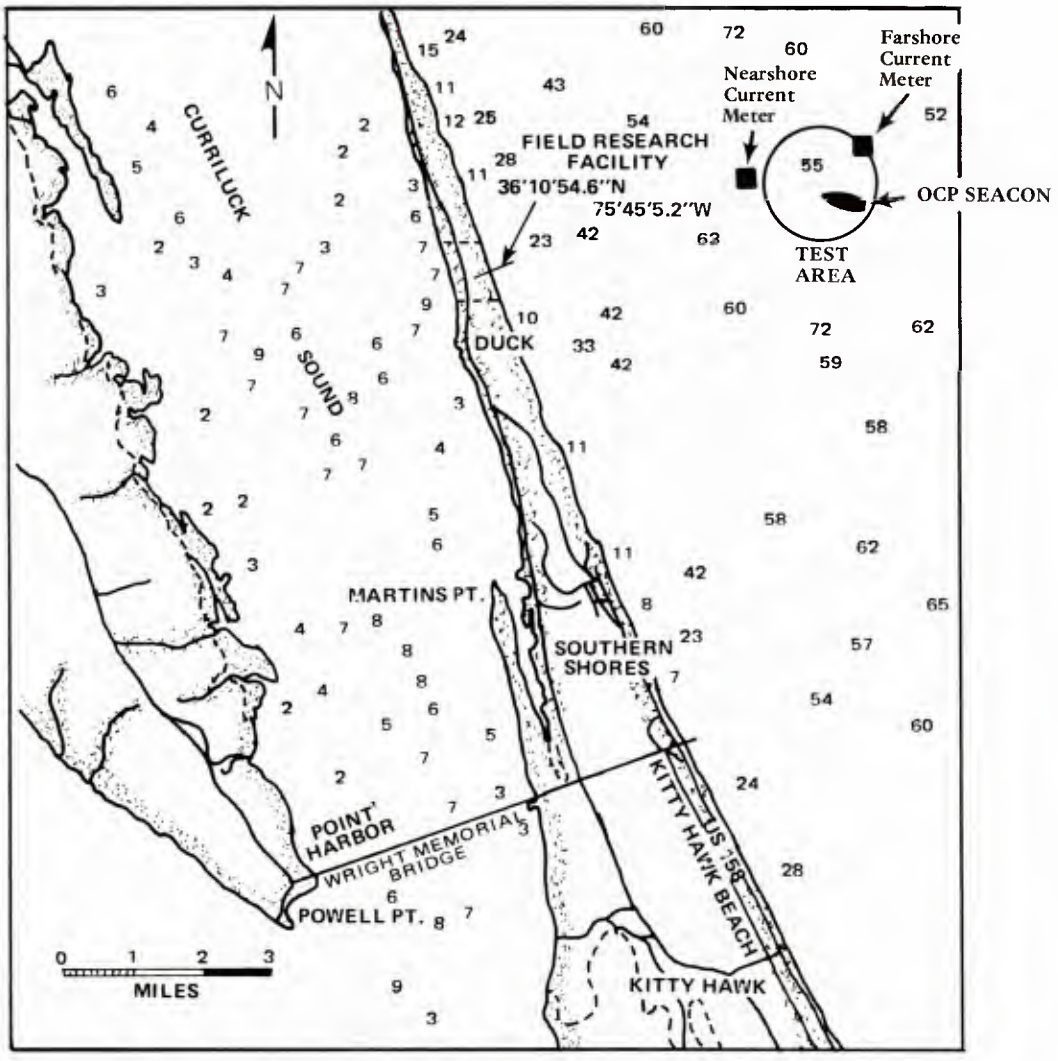

Figure 2. Location of MVE Ocean Tests.

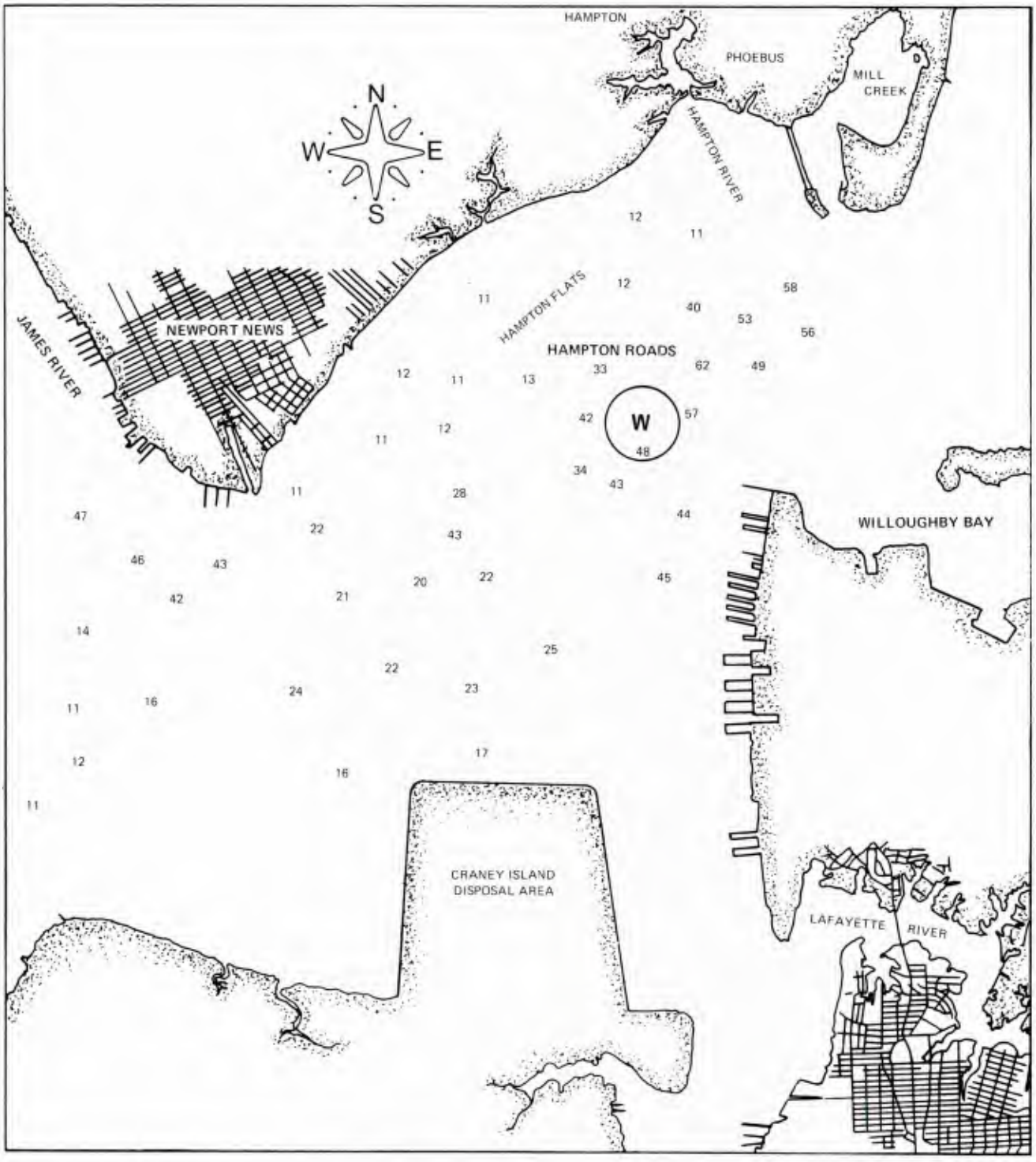

Figure 3. MVE wind and current test site.

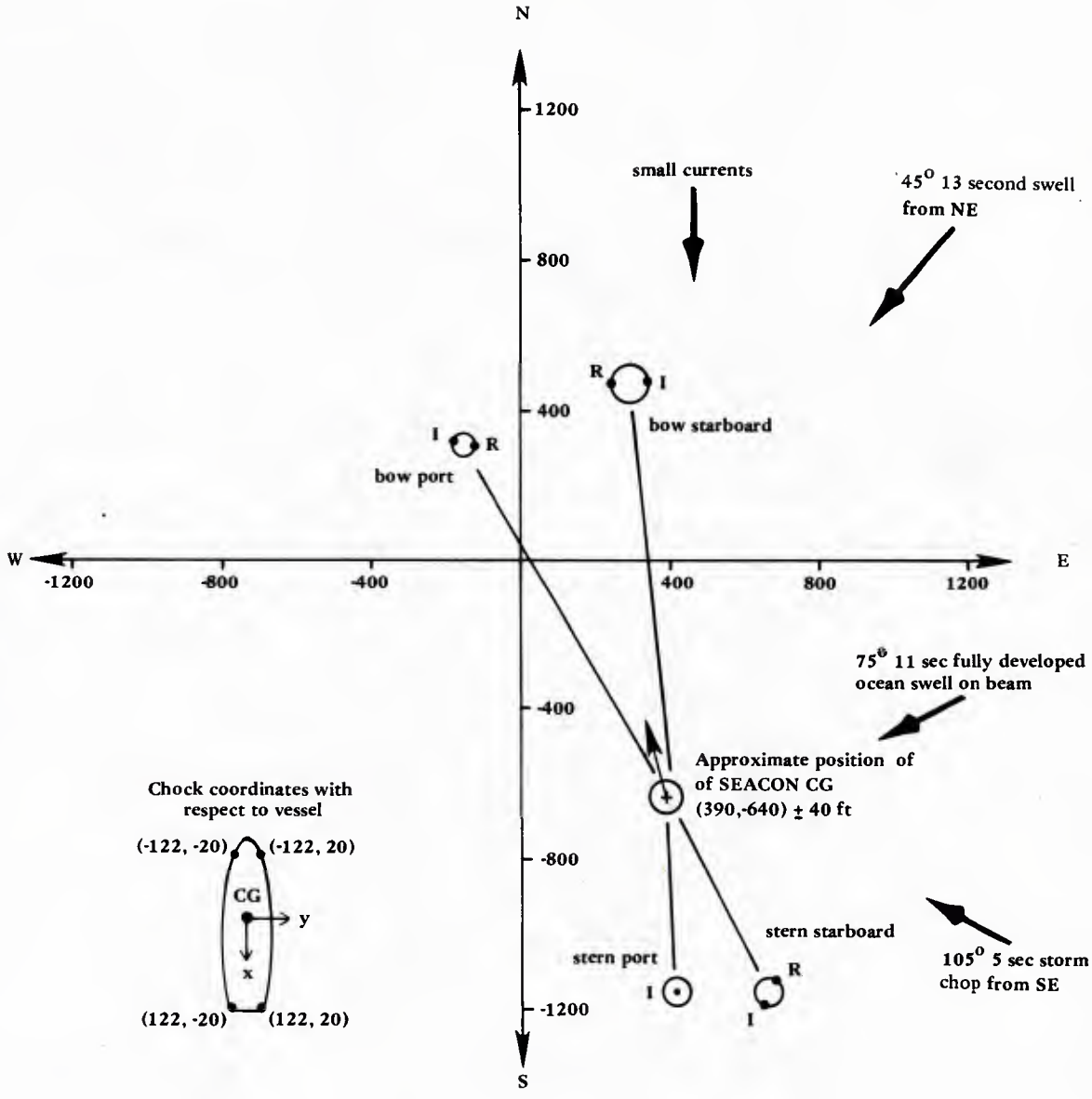

Figure 4a. Four-point mooring test configuration.

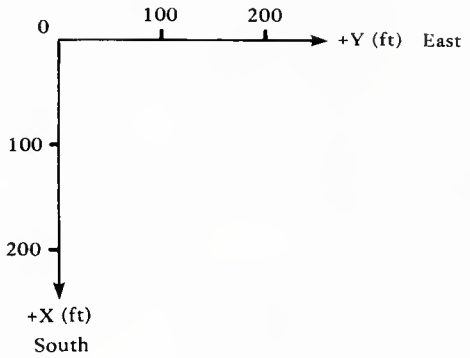

Anchor	(X, Y) coordinate (ft)		Drag Distance (ft)
	Installed (●)	Retrieved (o)	
1	-288, -190	-315, -141	56
2	-459, -367	-308, 439	167
3	1188, 748	1099, 672	117
4	1099, 387	1050, 371	51

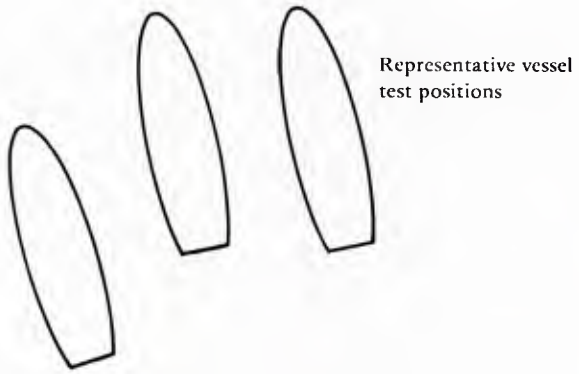

Figure 4b. Measured anchor coordinates.

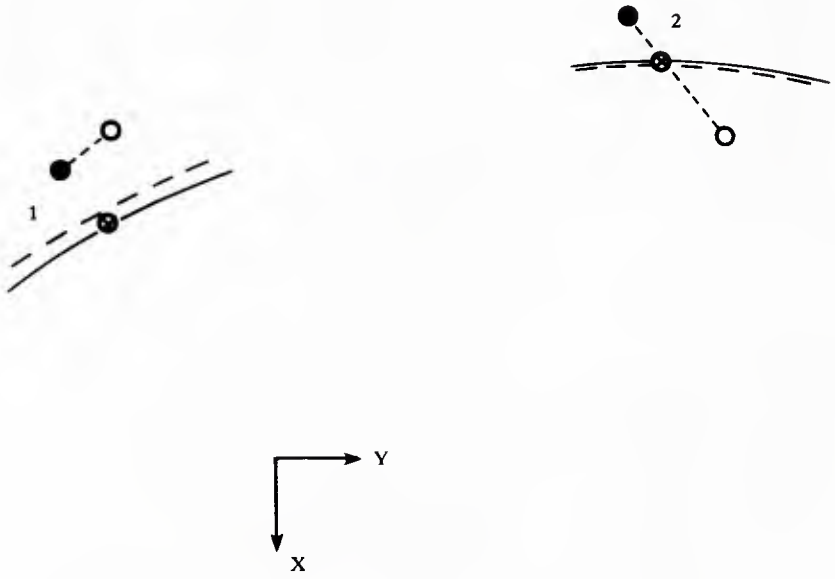

Leg	Line Lengths (ft)	
	Slack Tests	Taut Tests
1	978	958
2	1000	1000
3	407	407
4	357	346

Taut and slack test mean vessel positions

Representative taut test locus and vessel

Representative slack test locus and vessel

Reference Anchor Coordinates

- Released from vessel
- Retrieved
- Selected position for validations

Figure 4c. Anchor coordinates for the 4-point mooring tests.

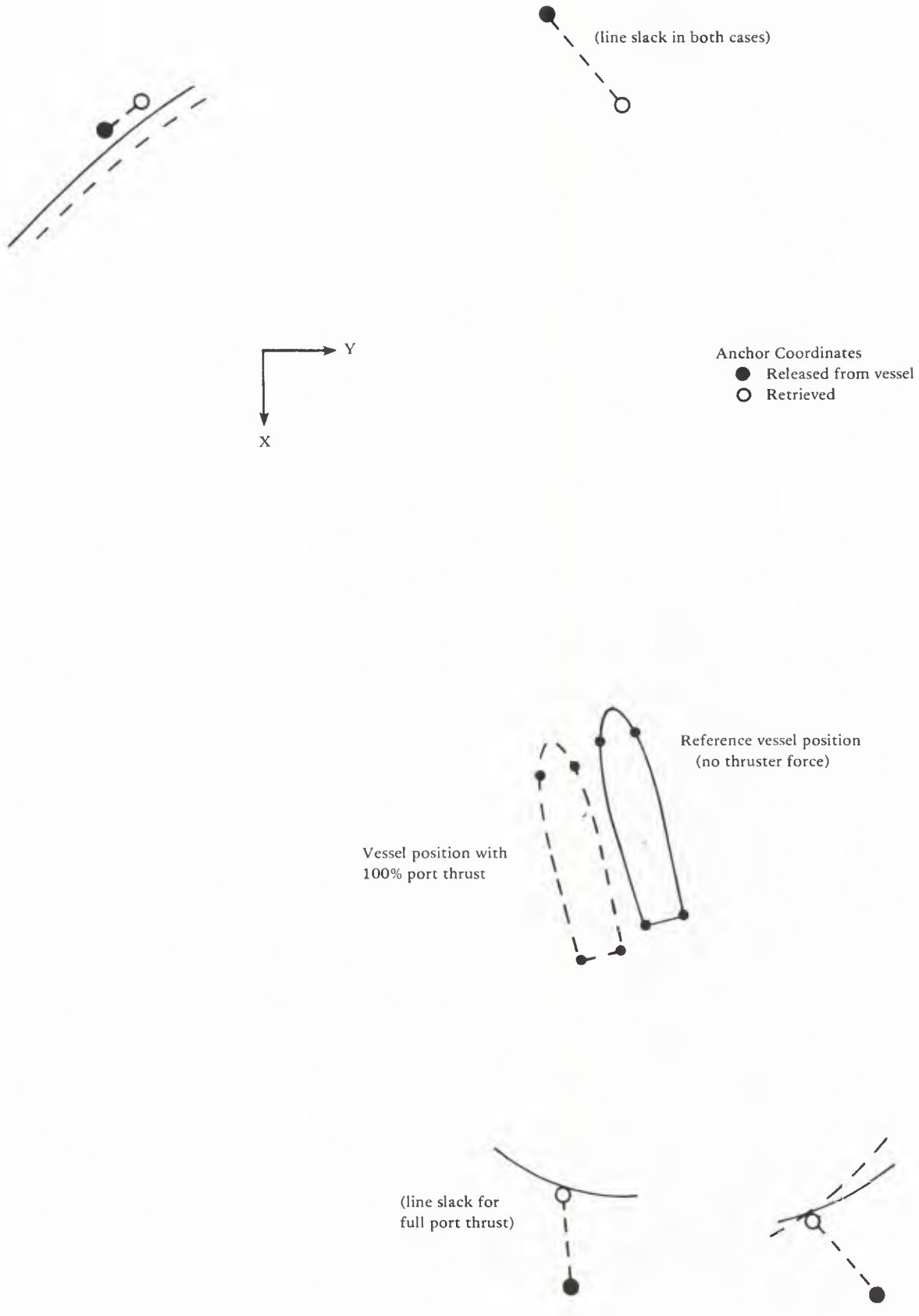

Figure 4d. Anchor coordinates for the static watchcircle tests.

N = Data points
XBAR = Mean value
SIGMA = Standard deviation
*Represents a Guassian distribution curve.

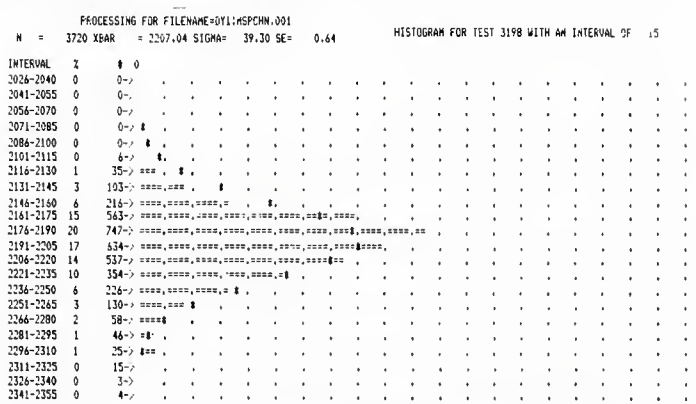

Bow Port Tension

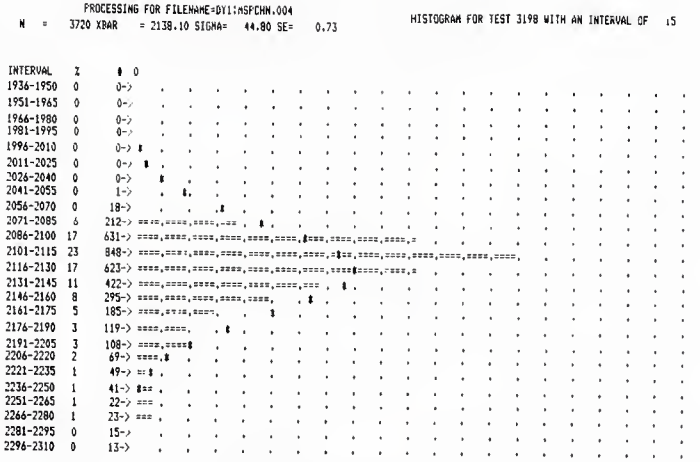

Bow Starboard Tension

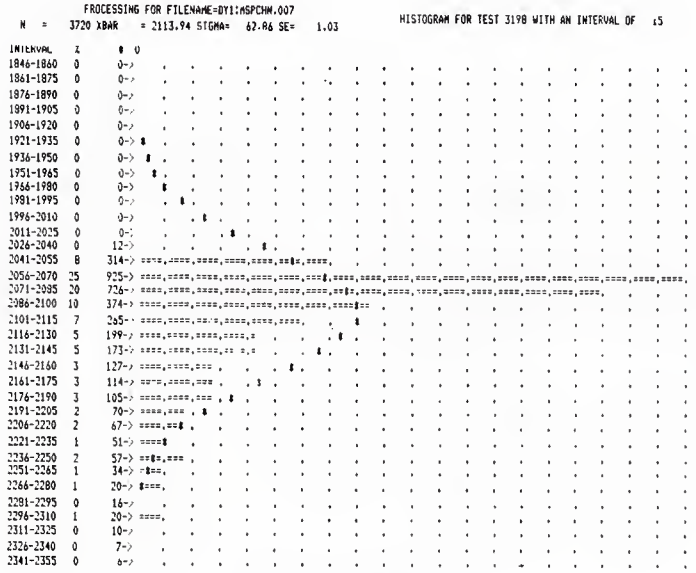

Stern Port Tension

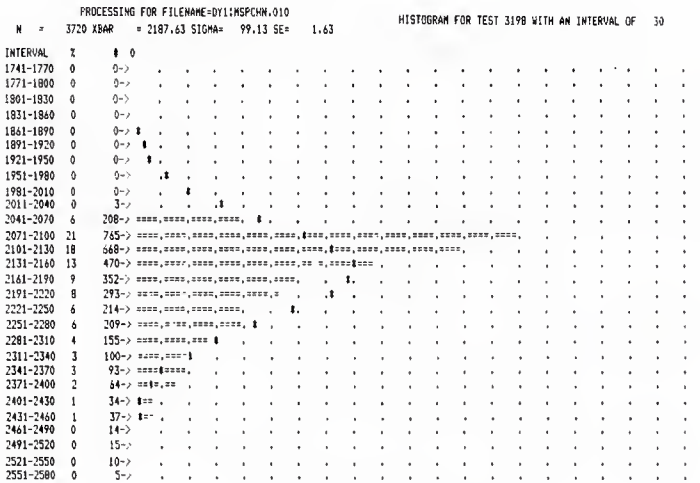

Stern Starboard Tension

Figure 5. Four-point mooring line tension distribution.

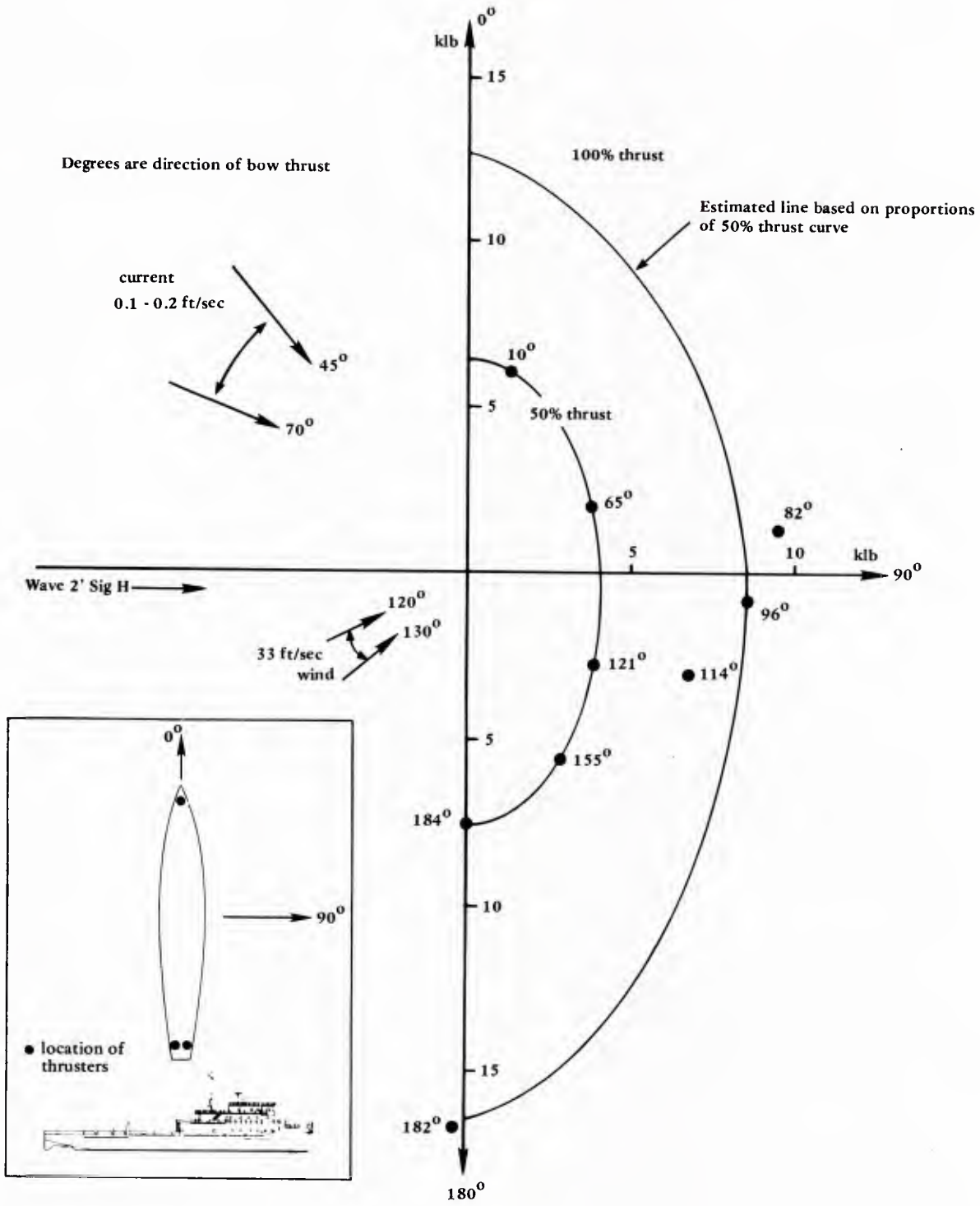

Figure 6. MVE Static Watchcircle Data.

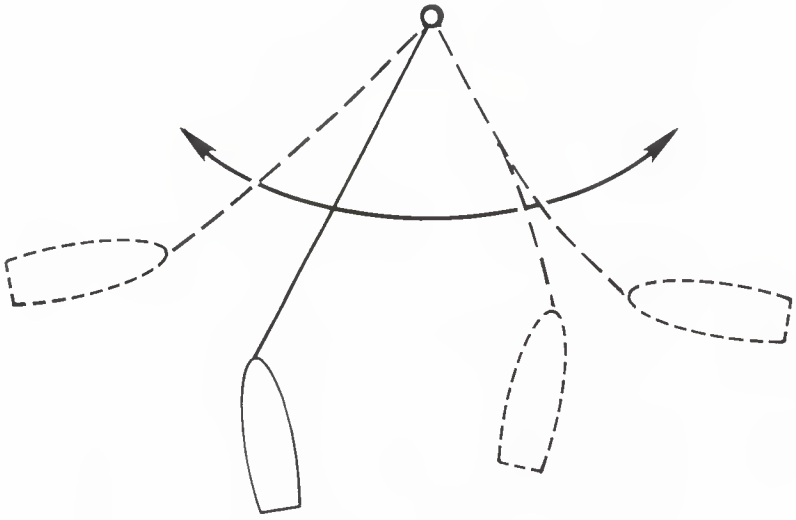

Figure 7. Single-point mooring test configuration.

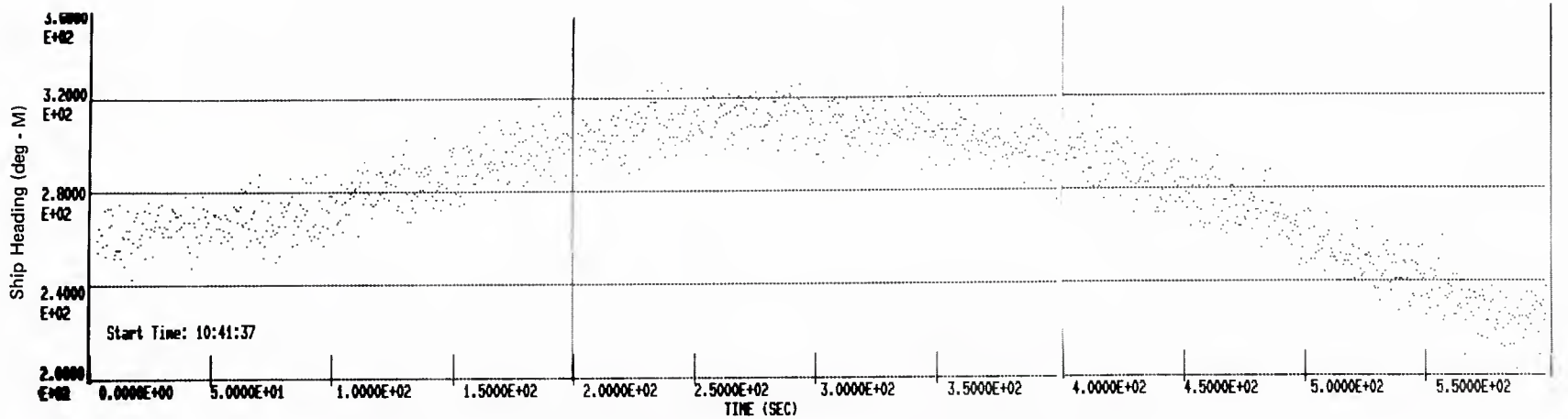

Figure 8. Ship heading (deg) vs time for Single Point Mooring tests.

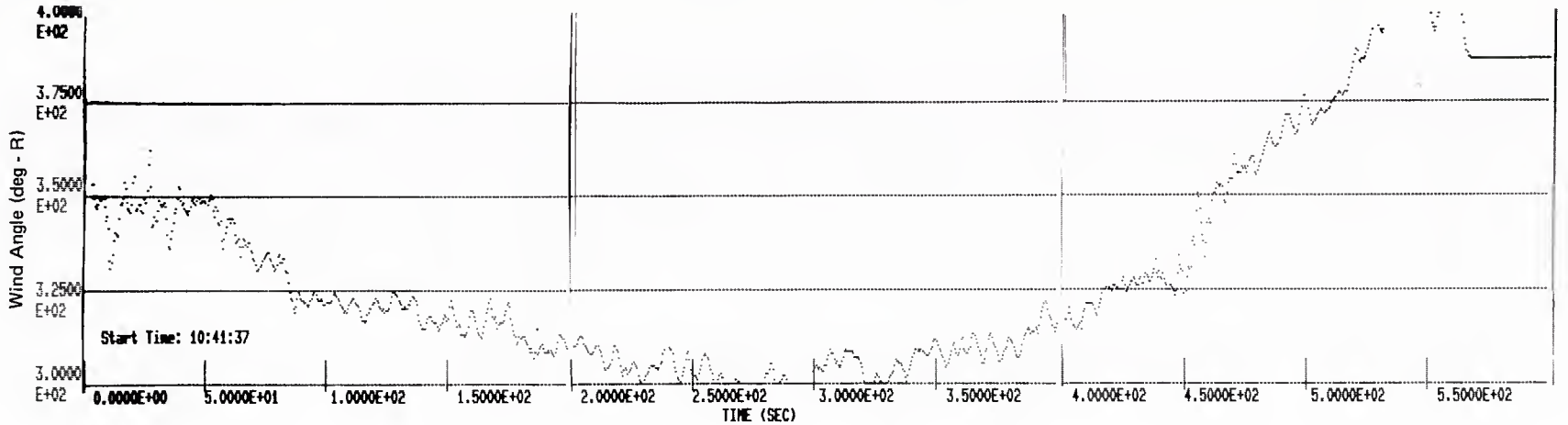

Figure 9. Relative wind angle (deg) vs time for Single Point Mooring tests.

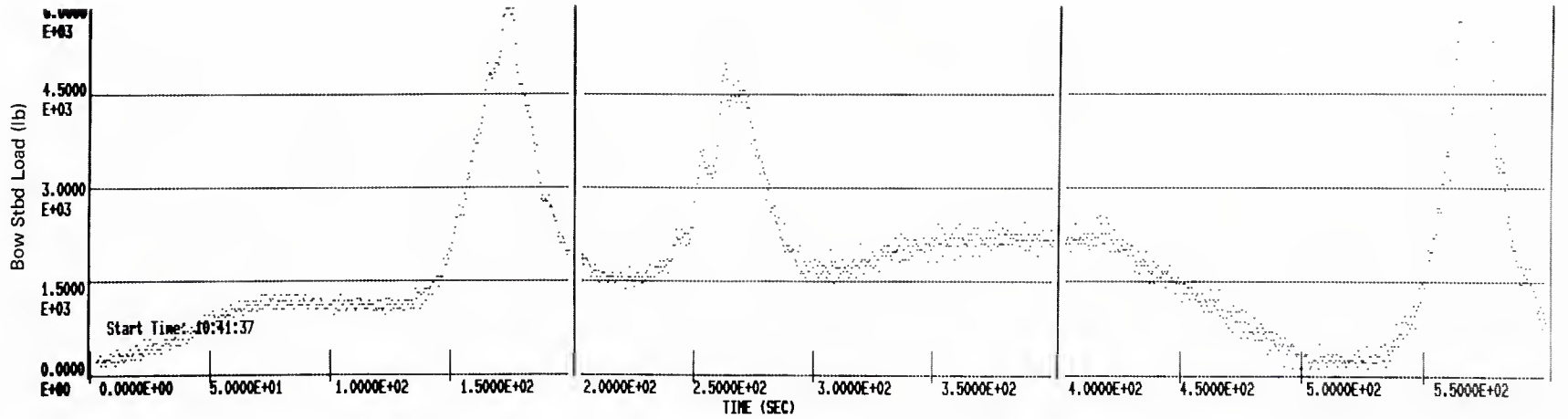

Figure 10. Hawser Tension (lbs) vs time for Single Point Mooring tests.

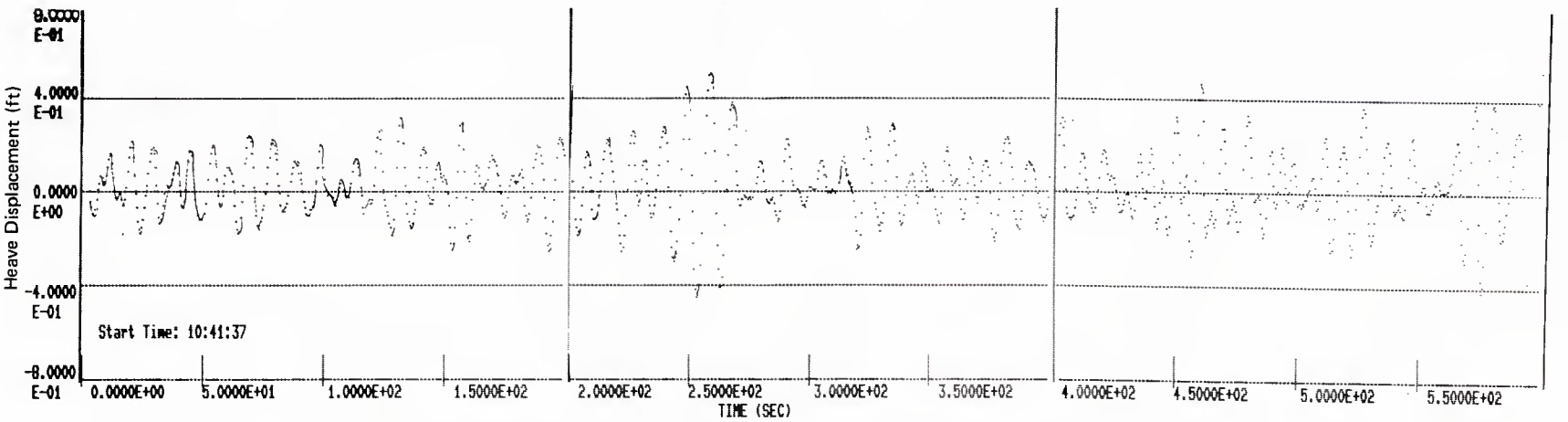

Figure 11. Heave displacement (ft) vs time for Single Point Mooring tests.

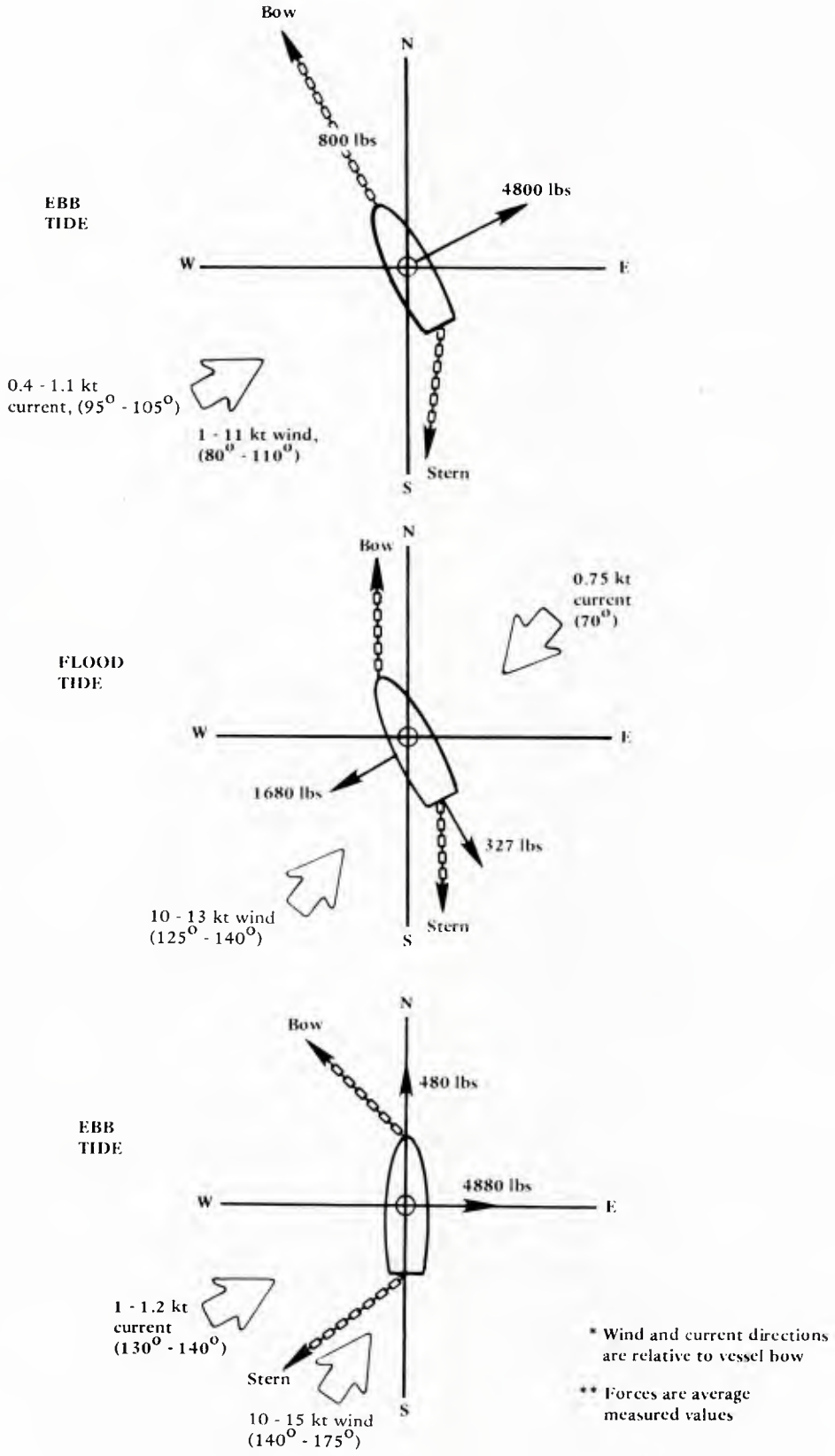

Figure 12. Wind and current test mooring configurations and environmental forces.

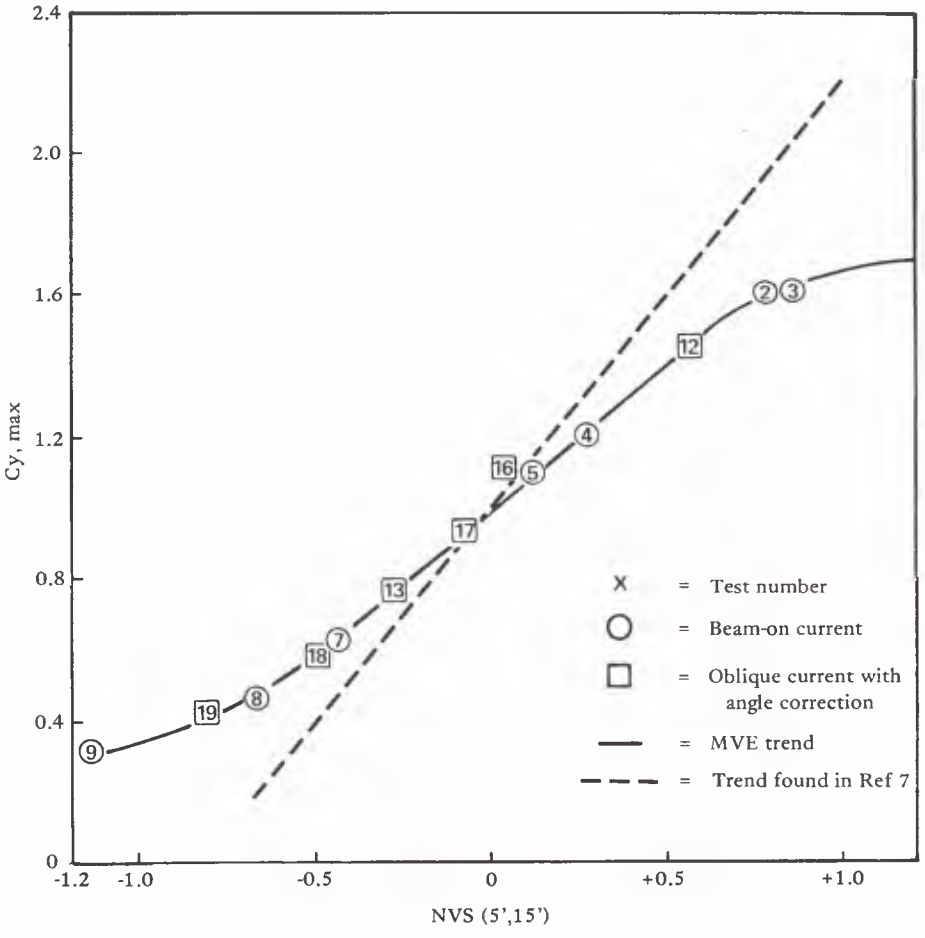

Figure 13. Lateral current force coefficient vs normalized current shear for the steady wind and current tests.

Appendix A

WAVE MEASUREMENTS

Two Waverider buoys were used to measure wave excitations in the immediate vicinity of the SEACON at the Mooring Validation Experiment (MVE) test site at Duck, NC (see Figure A-1). The purpose in recording data for two wave buoys and the mooring system was to measure the correlation (and coherence) between the two wave buoys and between a wave buoy and the mooring system.

Reference 6 describes correlation and coherence functions as follows. A cross-correlation function of two random time history records describes the general dependence of one set of data on the other. The cross-spectral density function is then the Fourier Transform of the cross-correlation function and is generally a complex number (includes phase information). This cross-spectral density information is also used to define a scalar (real-valued) parameter called the coherence function. The coherence is a normalized function that varies between 0 (no correlation) and 1.0 (perfect correlation-deterministic).

Two wave buoys were used to allow for elimination of wave translation effects in the wave buoy-system frequency response function calculations. The coherences between the two wave buoys and between the (closest) wave buoy and the mooring system were calculated from the time history records Theoretically, the coherence between the two wave buoys for a small-amplitude, deep-water, two-dimensional wave field would be 1. In actuality, the coherence is less than 1 between two points and is dependent upon the separation distance vector (parallel and perpendicular to the energy propagation direction(s)) and wave period. There is also a system coherence loss between the wave field (at the vessel) and the mooring responses since wave energy is not transferred linearly or with total efficiency into the vessel. The calculated wave propagation coherence is assumed stationary (a valid assumption); it can then be theoretically "subtracted" from the calculated wave-to-mooring-system coherence, thus eliminating effects due to wave translation between the buoys and the vessel. The resulting coherence is the wave-to-mooring-system coherence (e.g., vessel response amplitude operators (RAOs)).

The buoys were equally spaced from each other and the vessel and oriented in-line with the apparent incident wave angle and the vessel center. This placement was determined from the results of a previous Field Research Facility (FRF) test, sponsored by the Naval Civil Engineering Laboratory (NCEL), to determine the spatial coherence of random wave fields at this same site (Ref 9). In that study, approximate expected coherence values between two sensor positions in a unidirectional wave field were calculated as a function of parallel and perpendicular separation distance relative to the incident wave angle. This separation is defined in Figure A-2. The coherence function versus nondimensional

separation distance for unidirectional wave trains at this site is shown in Figure A-3, with smoothed contours of estimated maximum-attainable coherence added to aid interpretation.

Figure A-3 shows how quickly wave coherence decreases with separation along the crests (Y) compared to the direction of wave propagation (X). This demonstrates the importance of wave buoy placement in full-scale ocean experiments like the MVE. The buoy orientation of the MVE was selected to keep the crest separation low (buoys oriented in-line with waves approaching the vessel). The buoy-buoy and buoy-vessel separation was intended to be equal; Figure A-1 shows that this was generally achieved. This finite separation distance is a necessary compromise between: (1) minimizing the distance to minimize coherence loss (see Figure A-3), (2) staying far enough away from the hull to avoid measuring radiated and reflected waves, and (3) assuring that dynamic vessel excursions would not reach the buoy and damage it.

The buoy placement has two important consequences. First, the coherence between buoy No. 1 and buoy No. 2 is statistically equal to the coherence between buoy No. 1 and the undisturbed waves at the vessel (see Figure A-1). This is based on the standard assumption of stationarity of the wave field and is labeled the "wave propagation" coherence. Note that a calculated coherence between measured waves and any system response to these waves (e.g., heave RAO) is actually an effective coherence because it is the product of the wave propagation coherence and the system response coherence. Thus, the system coherence can theoretically be obtained by dividing the effective coherence by the wave propagation coherence. Figure A-4 shows a typical wave propagation coherence plot from the MVE test. The scatter evident in Figure A-4 was due to the low number of samples per test. This low number was limited by the (angular) nonstationarity of the incident wave field. This nonstationarity and the superposition effects of the two (or more) wave trains limited the effectiveness of this analysis technique (and similar phase corrections) in this application. The consequences of these measurements will be discussed in the subsequent validation report.

The second consequence of using two buoys is that it allows for a reasonable estimation of the incident wave field directions as follows:

1. Calculate the theoretical shoaled wave length at each frequency.

2. Select a trial wave angle, and calculate the component of the parallel buoy separation distance (apparent wave length for that oblique (relative to the wave direction) buoy placement).

3. Calculate the theoretical phase difference for that frequency from the ratio of the effective to actual wave lengths.

4. Compare this theoretical phase to the measured phase; iterate until convergence.

Figure A-5 and Table A-1 illustrate how the parallel separation distance is calculated for several incident angles. Table A-1 lists the theoretical phase difference between the two wave buoys for various incident angles and frequencies. These theoretical phases are plotted

against the measured phase differences in Figure A-6. Figure A-7 shows the wave autospectrum for the same test; the two peaks indicate the presence of two wave trains.

Figures A-8a, b, and c are plots of the theoretical minus the measured phase for three trial incident wave angle pairs, which demonstrates the level of convergence explained in step 4 above. (Two trial angles are specified relative to the 110° orientation of the wave buoys because of ambiguity in resolving the phase, as shown in Figure A-5. Also note that the values are relative to the zero line--black above, white below.) Inspection shows that the plot for 70/150 wave incidence (Figure A-8b) has the smallest phase difference for the fully-developed wave train, indicating an incident angle of 150° (true) for this particular test. This agrees well with the measured incident angle of 140°. (The same effect occurs for an incident wave angle of 70° (true), but this was discarded as inconsistent with the observed wave angle.) For the higher frequency wave train shown in Figure A-7, inspection of Figure A-8 shows that the best phase agreement corresponds to a relative incident angle of 130° (Figure A-8a), which is also in good agreement with the observed incident angle of 140°. Also note a third distinct wave train between 0.03 and 0.06 Hz, corresponding to a narrow swell field.

Summarizing, the information from two wave buoys has been shown to be useful if not necessary for proper interpretation of full-scale stochastic data with a finite buoy-system separation. This simple procedure was used to identify wave angles that agreed with the direct (radar) measurements and observations. It is, therefore, concluded that the information available from using two well-placed wave buoys is an interesting and worthwhile addition to full-scale testing.

Table A-1. Theoretical Phase Difference Between Buoys No. 1 and No. 2

Period (s)	Δf[a]	55-ft Depth Shoaled Wave length (ft)	Theoretical Phase Difference (°) at Incident Wave Angles of--			
			±5°	±20°	±40°	±60°
16.5	31	666	129	122	99	64
11.1	46	426	202	190	155	101
8.0	64	278	310	291	238	155
6.5	79	202	66	41	328	214
6.0	85	178	123	95	12	243
5.6	91	158	185	153	60	273
5.1	100	133	287	249	138	325
4.7	110	110	62	76	242	33
4.0	128	83	317	256	78	160

[a]Graphs list frequencies by multiples of the bandwidth ($\Delta f = \frac{1}{512}$ Hz).

For example, for f = 0.10 Hz = $\frac{51.2}{512}$ Hz, then $\Delta f = 51.2$

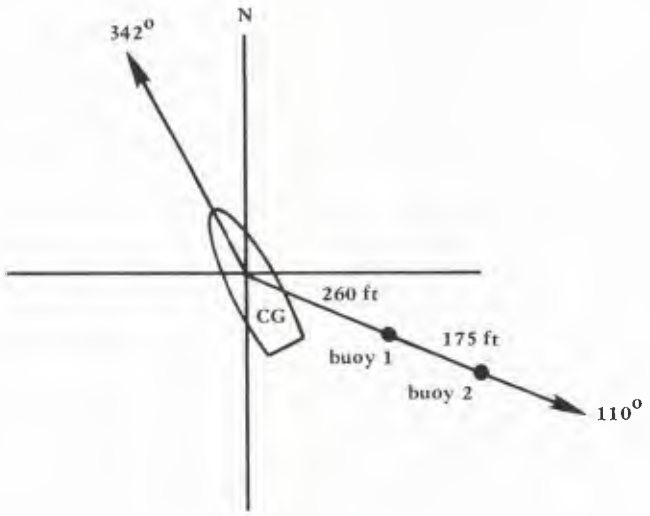

TEST 1

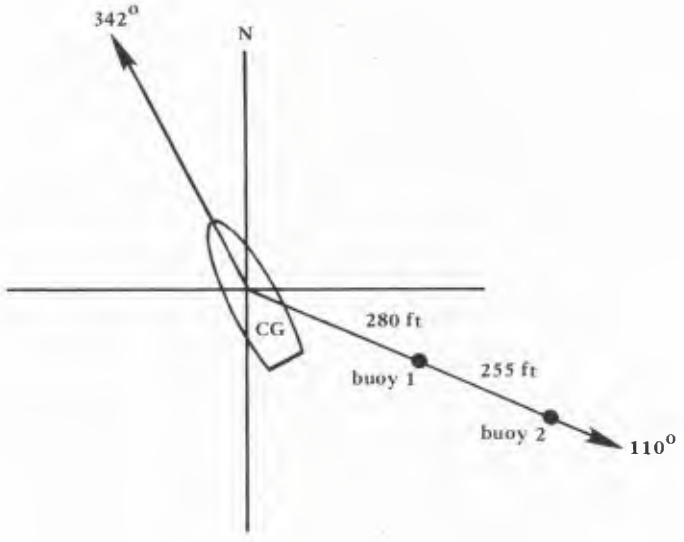

TEST 6

Figure A-1. Four-point mooring test; waverider buoys location.

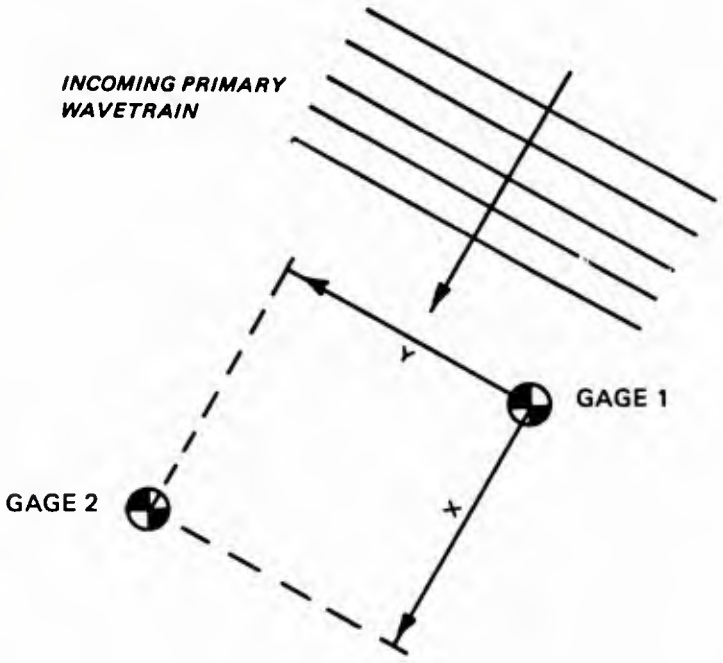

(a) Primary wave direction

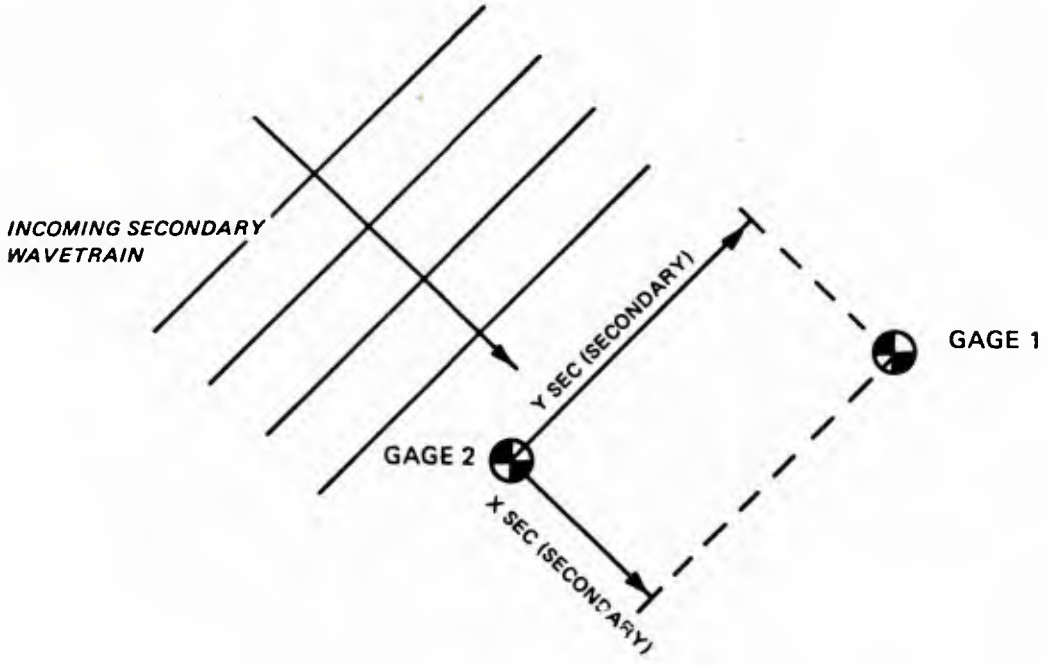

(b) Secondary wave direction

Figure A-2. Definition of parallel (along-crest) and perpendicular (down-crest) distances for two simultaneous incident wave fields.

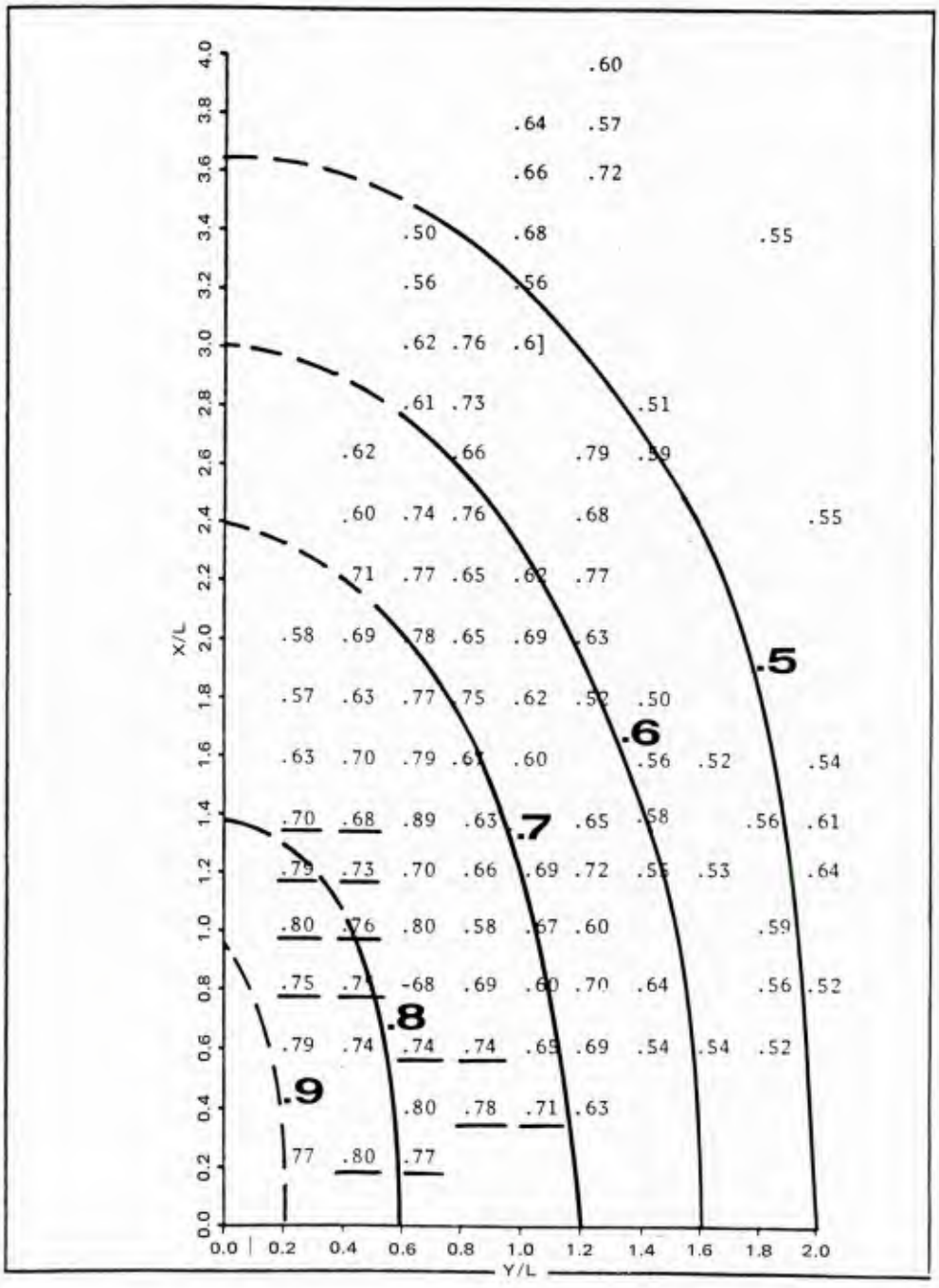

x = distance between sensors parallel to wave direction
y = distance between sensors perpendicular to wave direction
L = wave length

Figure A-3. Nondimensional coherence coutours for shallow water (17 m).

Note: A coherence between 0.5 and 1.0 is considered significant.

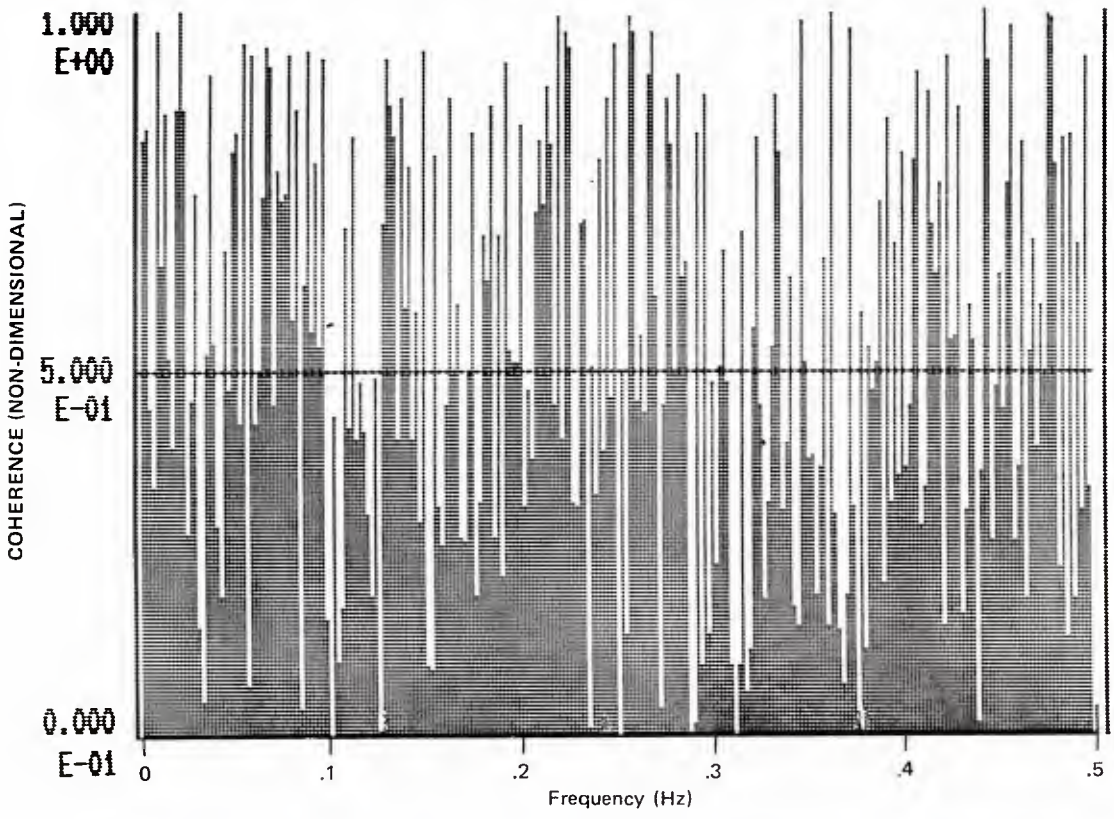

Figure A-4. Coherence between buoy #1 and #2 for four-point mooring test #4.

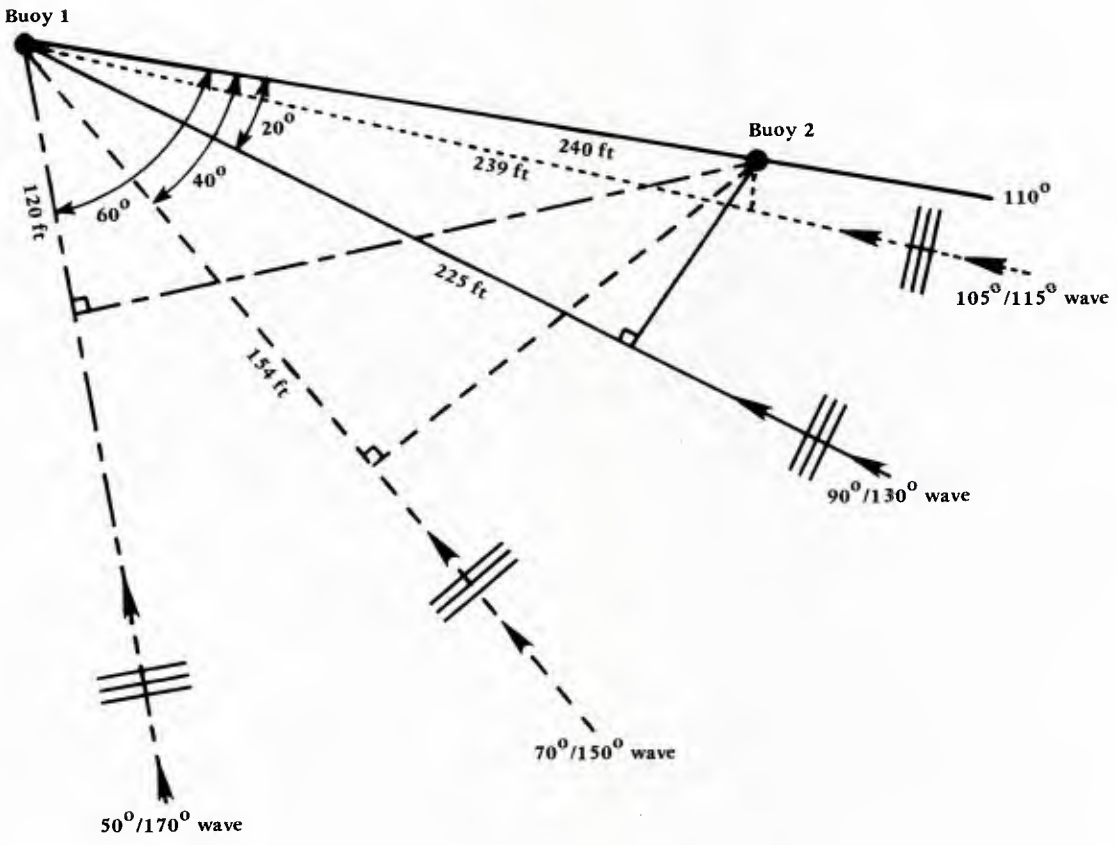

Figure A-5. Effect of wave angle incidence on phase difference between wave buoys.

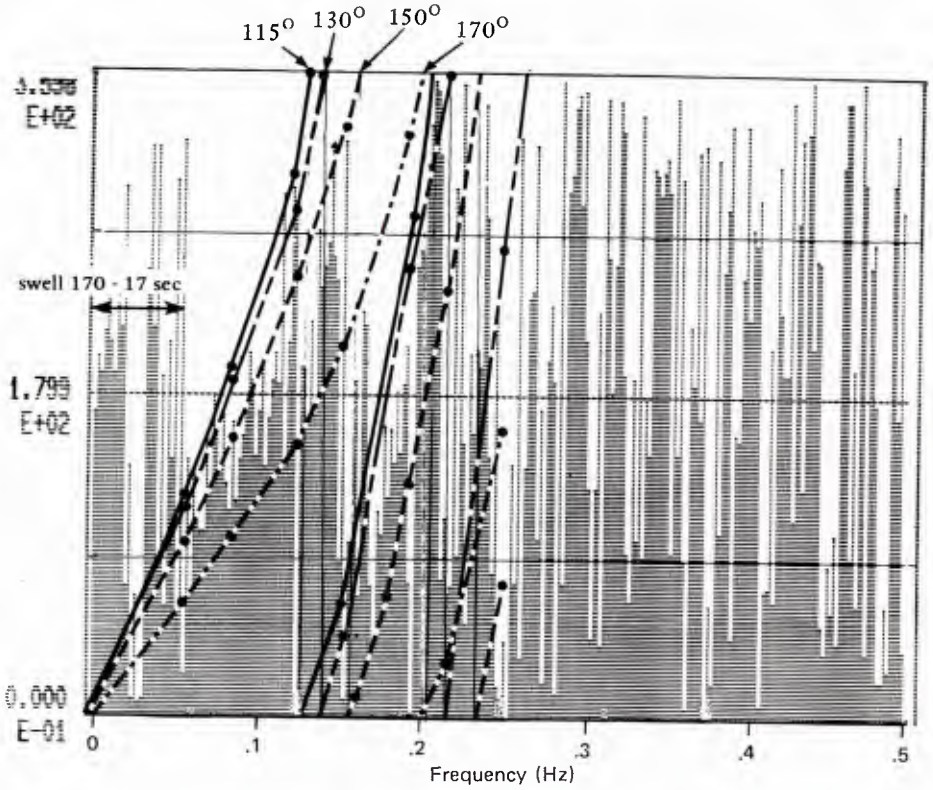

Figure A-6. Phase difference between Buoy 1 and 2 vs wave frequency (lines show theoretical phase difference for angle of incidence).

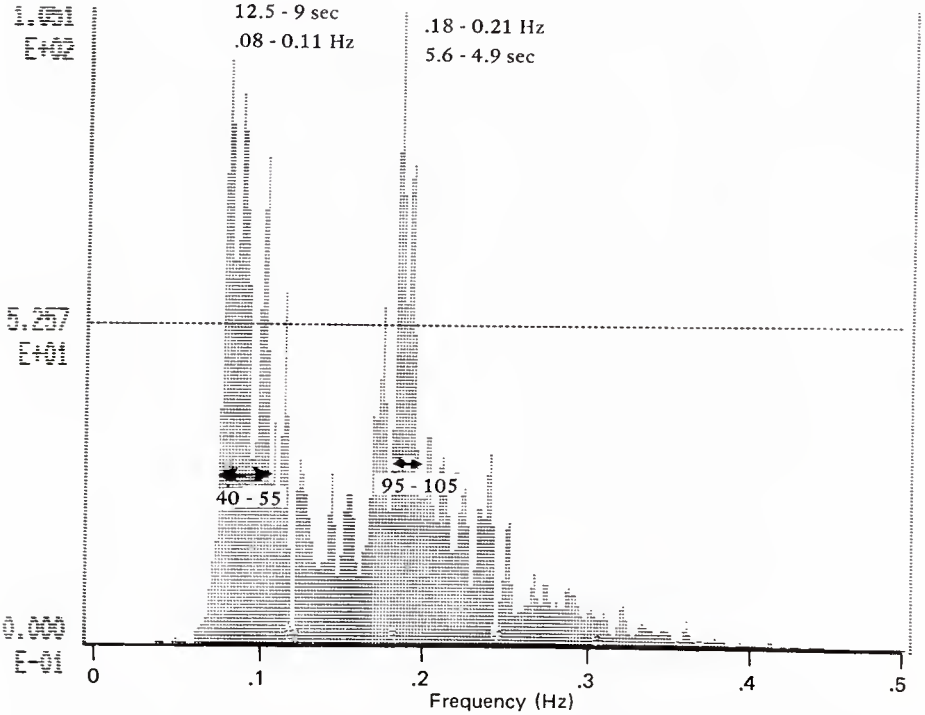

Figure A-7. Wave buoy # 2 Autospectrum for four-point mooring test # 8.

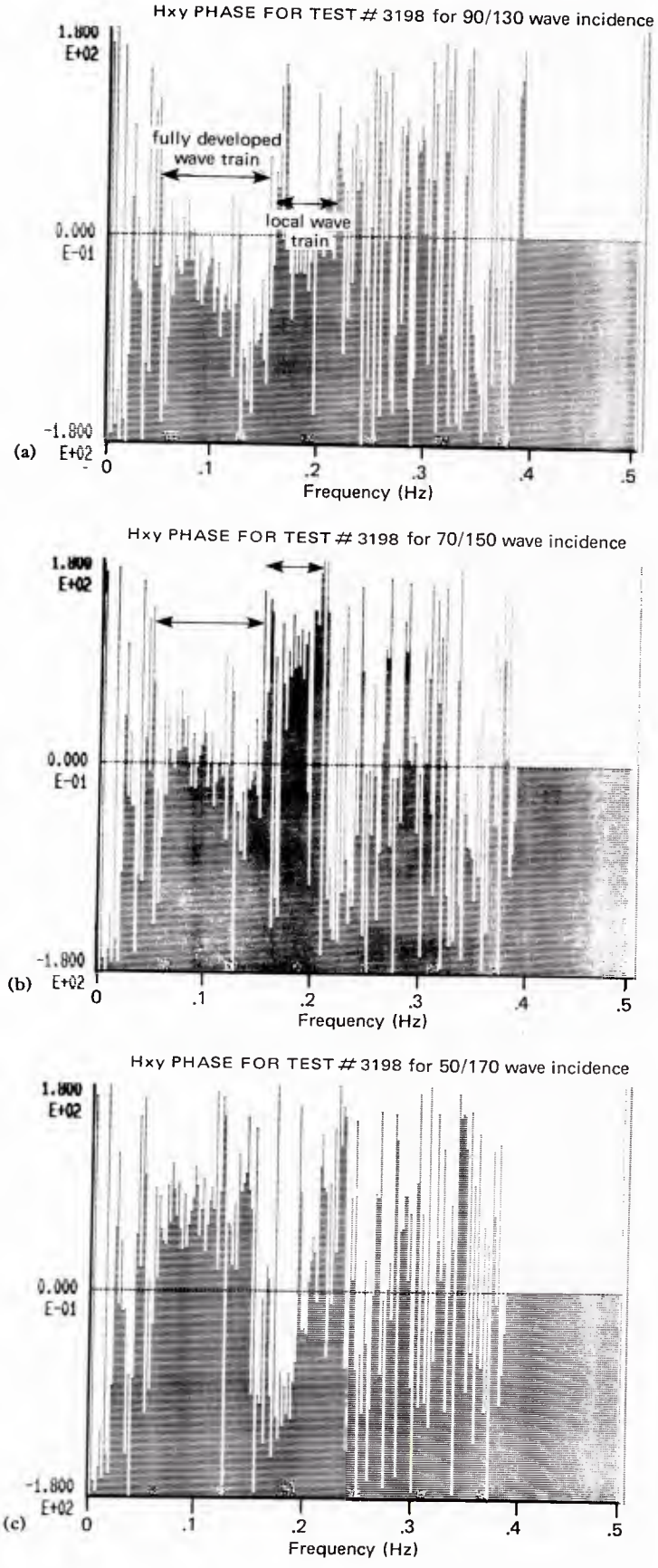

Figure A-8. Difference between theoretical and measured phases for various trial incident wave directions, as shown in Figure A-5.

Appendix B

SUMMARY OF ENVIRONMENTAL CONDITIONS DURING THE MOORING VALIDATION EXPERIMENT AT DUCK, NC (taken from Ref 5)

SUMMARY

Between 14 and 17 November 1983, the SEACON was exposed to the following conditions:

Date and Time	Winds	Waves	Near-Surface Current
1700 14 Nov - 0200 15 Nov	Light (0.7 ft/s)	Low (1.3 ft)	Large (1.6 ft/s)
0200 15 Nov - 2400 15 Nov	High (33 ft/s)	Medium (4.9 ft)	Large (1.6 ft/s) to small (0.3 ft/s)
0000 16 Nov - 1200 16 Nov	Medium (16 ft/s)	Medium (3.3 ft)	Small and variable
1200 16 Nov - 1200 17 Nov	High (33 ft/s)	Low	Medium (0.7 ft/s)

INSTRUMENTATION

Four wave gauges were used to measure the wave field. Baylor staff inductance wave gauge at the seaward end of the FRF research pier and Waverider buoy wave gauge north of the ship (Figure B-1) provided basic wave height and period data throughout the experiment. However, to determine the wave field at the ship's exact position, two other Waveriders were positioned in close proximity to the ship.

Neil Brown acoustic current meters were placed on taut wire moorings about 1,000 feet on either side of the vessel (Figure B-1). The LARC-V was used to deploy the moorings, and a Zeiss electronic total station was used for positioning the craft. At the primary (nearshore) mooring (water depth = 54.5 feet mean sea level (MSL), one meter was positioned at a depth of 14.5 feet MSL and a lower one was positioned at a depth of 29 feet MSL. These meters were designed to sample current speed and direction every second for 15 minutes, determine the resultant speed and direction for that 15-minute sample, and write the data on an internal cassette tape.

An anemometer on the FRF office building provided wind speed and direction data, and visual observations were made of wave direction (including radar-measured waves), currents at the pier end and in the breaker zone, and other oceanographic parameters (water temperature, visibility, etc.).

DATA REDUCTION AND ANALYSIS

Figure B-2 shows the time history of hourly values of wind speed and direction.

Data from the pier-end Baylor gauge and the Waverider were analyzed using a Fast Fourier Transform analysis routine, which yields the band spectra (frequency versus percent normalized variance), a wave height parameter (four times the standard deviation of the record), and the period associated with the maximum energy density. Plots of the wave height and period time histories for both the Baylor and Waverider gauges are shown in Figure B-3.

Cassette tapes from the Neil Brown current meters were sent to a private company for reduction. Plots of the time histories of current speed and direction at the two nearshore current meters are shown in Figure B-4.

Upon return of the data printouts to the FRF, it was noticed that directional data from the farshore current meter did not agree with those from the nearshore meters. As a result of questions posed to the leasor of the equipment regarding the proper functioning, it was discovered that an incorrect circuit card had been emplaced in the farshore meter by the factory. Although the speeds indicated on each channel were correct, the directional characteristics could not be determined from the data because of uncertainties in the meter's orientation during each sample run. However, if the current direction could be assumed to be identical to that of the nearshore meters, and the meter orientation remained constant, then the magnitude could be determined. Such conditions occurred only between 1700 on 15 November and 0800 on 16 November.

RESULTS OF ENVIRONMENTAL MEASUREMENTS

The following discussion presents an assessment of the forces affecting the ship during the SEACON's 3-day deployment (1500 on 14 November through 1700 on 17 November 1983). Since winds appear to be the primary factor controlling waves and currents during the experiment, their characteristics will be addressed first.

Between 1500 on 14 November and 0600 on 15 November, the wind speed remained constant at about 6.6 ft/s. However, the wind direction gradually rotated counterclockwise from due north on 14 November to about 135° (southeast) by 1000 on 15 November. Between 0600 and 1000 the speed increased drastically, reaching about 33 ft/s until 2000. The wind direction slowly changed from 135° (southeast) to 190° (southeast), but this time with a clockwise rotation. This process continued after 2000 as the wind speed gradually diminished, reaching a maximum of 300° (west-northwest) at 0600 on 16 November. At that time, the wind

speed began a gradual increase to about 39 ft/s and, after a relatively rapid shift of direction to about 270° (west) at 1100 on 16 November, the wind remained out of the west-northwest for the final 24 hours of the experiment.

Strong winds from the southeast on the morning of 15 November caused rapid development of wind waves such that by noon the significant wave height had reached a maximum of 4.9 ft (Figure B-3). As the winds shifted from the southeast to the west, wave heights decreased almost linearly, returning to their prestorm values of less than 1.6 ft by 2400 on 16 November. Wave spectra indicate that at 0700 on 15 November, the wave field could be characterized by a single-peaked spectrum (peak period about 7.5 seconds). Radar wave direction observations taken at that time indicate an offshore wave approach angle of 45° (relative to true north). By 1400, however, two wave trains were evident in the nearshore zone, one arriving from 75° and the other from 105°. The 75° train appeared to have the most energy (about 15 percent of the variance) at a period of about 11 seconds, while the 105° train contained about 9 percent of the variance at a period of about 5 seconds.

At 1700, only one train could be identified on the radar image, approaching from an angle of 95°. Corresponding visual observations of incident wave angle show the predominant seas from 140°. It is concluded that the radar technique missed the energy from this direction because the wave fronts were almost parallel to the radar site and showed little backscatter. However, wave image data obtained at 1900 indicate the continued existence of two wave trains, with peak periods of about 5.5 and 11 seconds. It is concluded that the long swell was incident from 95°, with all other energy incident from 140°; see Appendix A for additional wave direction estimates. By 0100 on 16 November, as wave heights began to decrease, only one wave train was evident from the spectral output (T = 11 s), a situation which continued throughout the remainder of the experiment. The visual observations indicate that waves on the morning of 16 November approached from an angle of 85°.

The current patterns indicated by this data set are extremely interesting yet quite complex. Since the ship's mooring system precluded placement of the current meters in close proximity to the ship, they were moored about 1,000 feet on either side. The currents at the test site are determined by interpolating between these two data sets.

The data shown in Figure B-4 provide current speeds and direction at the nearshore location at depths of 14.5 and 29 feet MSL. Although most of the data from the farshore meter were not retrievable, reliable estimates of current speeds for the 15-hour period on 15 to 16 November indicated that the currents affecting the ship should be adequately represented by the data from the nearshore near-surface meter.

Between 1800 and 2000 on 14 November, near-surface current speeds increased rapidly to over 1.6 ft/s, remained relatively constant until about 0900 on 15 November, and then decreased rapidly over the next 6-hours. Throughout most of this period, currents were flowing southward. This agrees well with the dye measurements obtained at 0700 on 15 November at the end of the FRF pier and in the midsurf zone under the pier, which both indicated a current of about 0.25 m/sec directed southward.

The time period between noon on 15 November and midnight on 16 November appears to be a transitional period for the currents, apparently in response to the rapidly changing wind regime. The near-surface current speeds were relatively low, averaging less than 0.3 ft/s.

Some tidal forcing is indicated in both meters' speed time series, with maximum and minima at the expected 12-hour spacing. However, the directional data show peculiar differences during this time period. Between noon on 15 November and 0600 on 16 November, the nearshore current varied between 180° and 80° at about 12-hour intervals.

In comparing the near-surface and middepth currents at the nearshore site, note that the middepth speeds were often smaller, while the directions were generally in very good agreement, except during the transitional period of 15 and 16 November.

The correlation between winds and currents at this location is rather complex. As the wind speed increased and its direction rotated counterclockwise early on 15 November, the current direction remained constant with depth (southward). However, between noon and midnight on 15 November, as the wind direction rotated clockwise, currents at the surface changed direction in a counterclockwise sense, while those at the bottom rotated clockwise. Such a difference in current patterns over such a small vertical distance (about 15 feet) is extremely puzzling. A thorough check of data quality shows no questionable data, so it appears that a shear zone existed for about 15 hours between the 15- and 30-foot depths at the nearshore site.

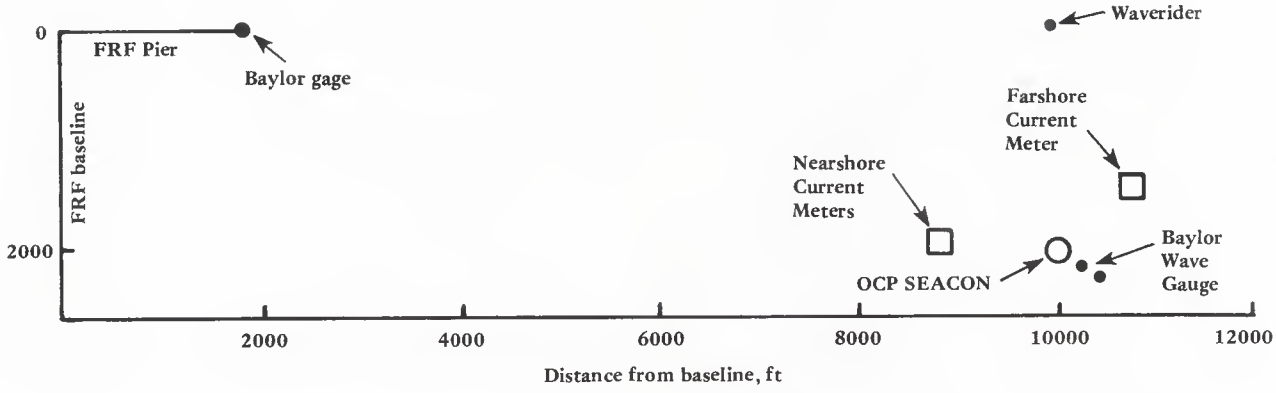

Figure B-1. Relative location of MVE environmental instrumentation.

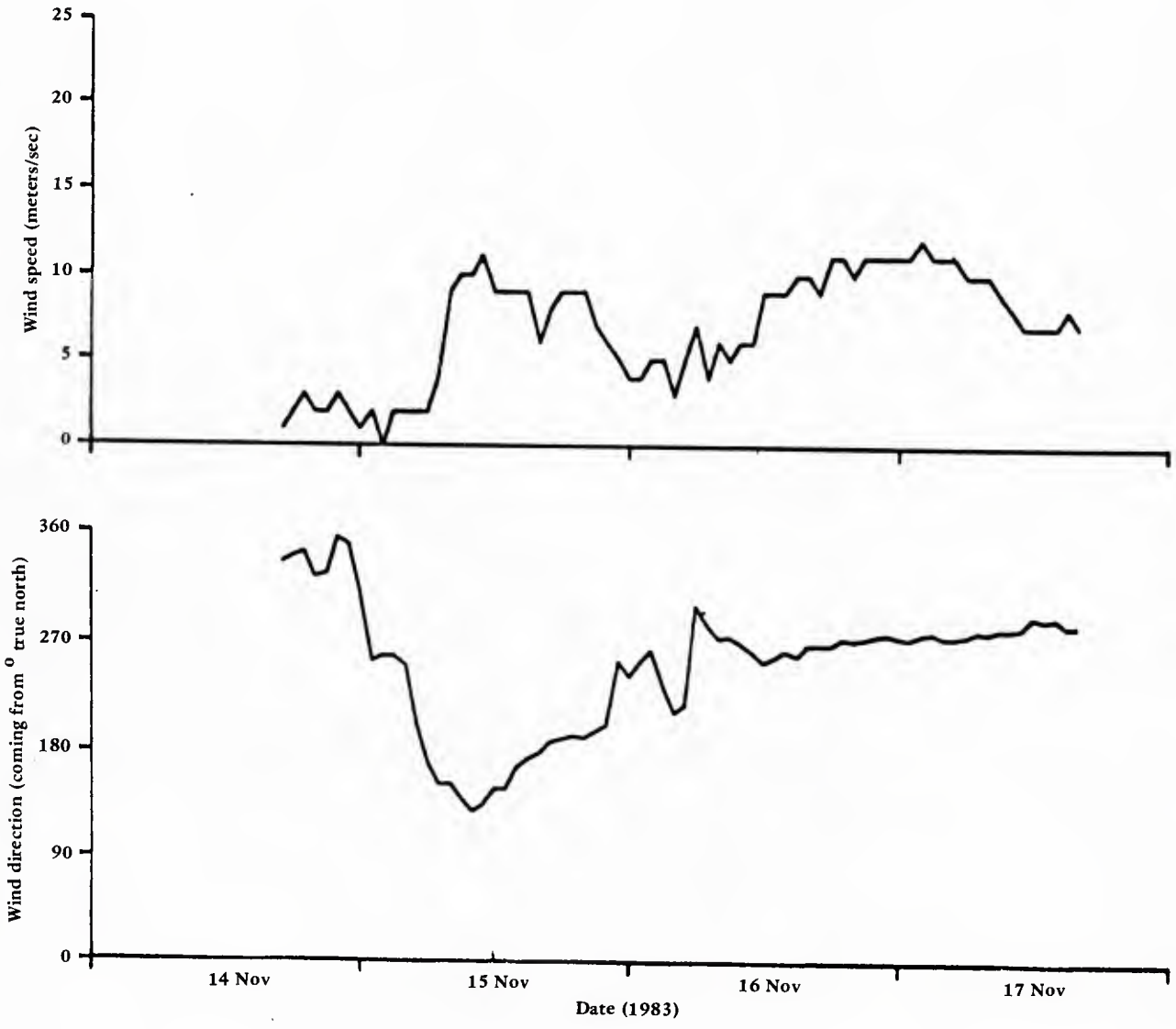

Figure B-2. Time history of wind speed and direction, FRF building anemometer, 14 - 17 November 1983.

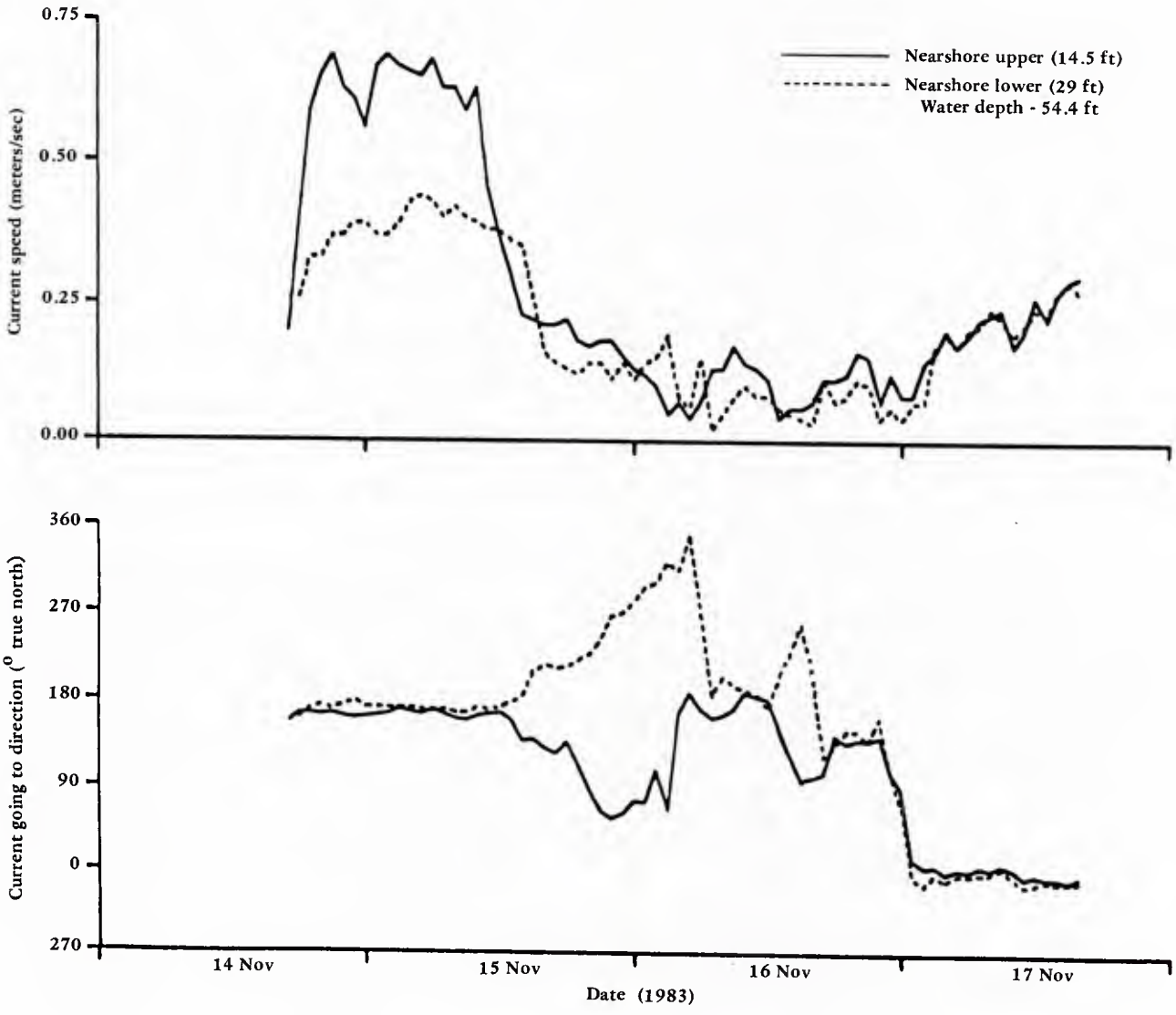

Figure B-3. Time history of current speed and direction, nearshore array, 14 - 17 November 1983.

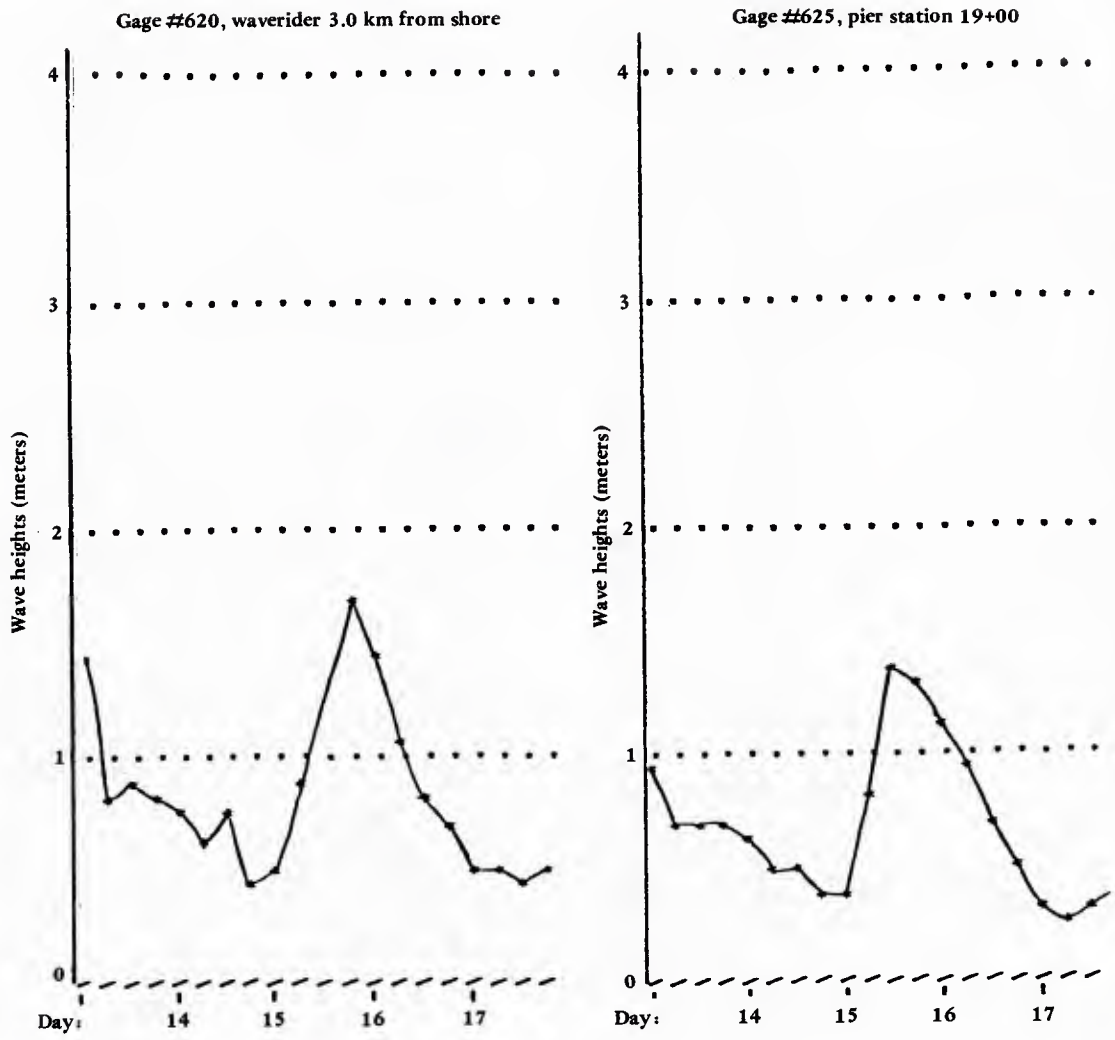

Figure B-4. Wave heights, 14 - 17 November 1983.

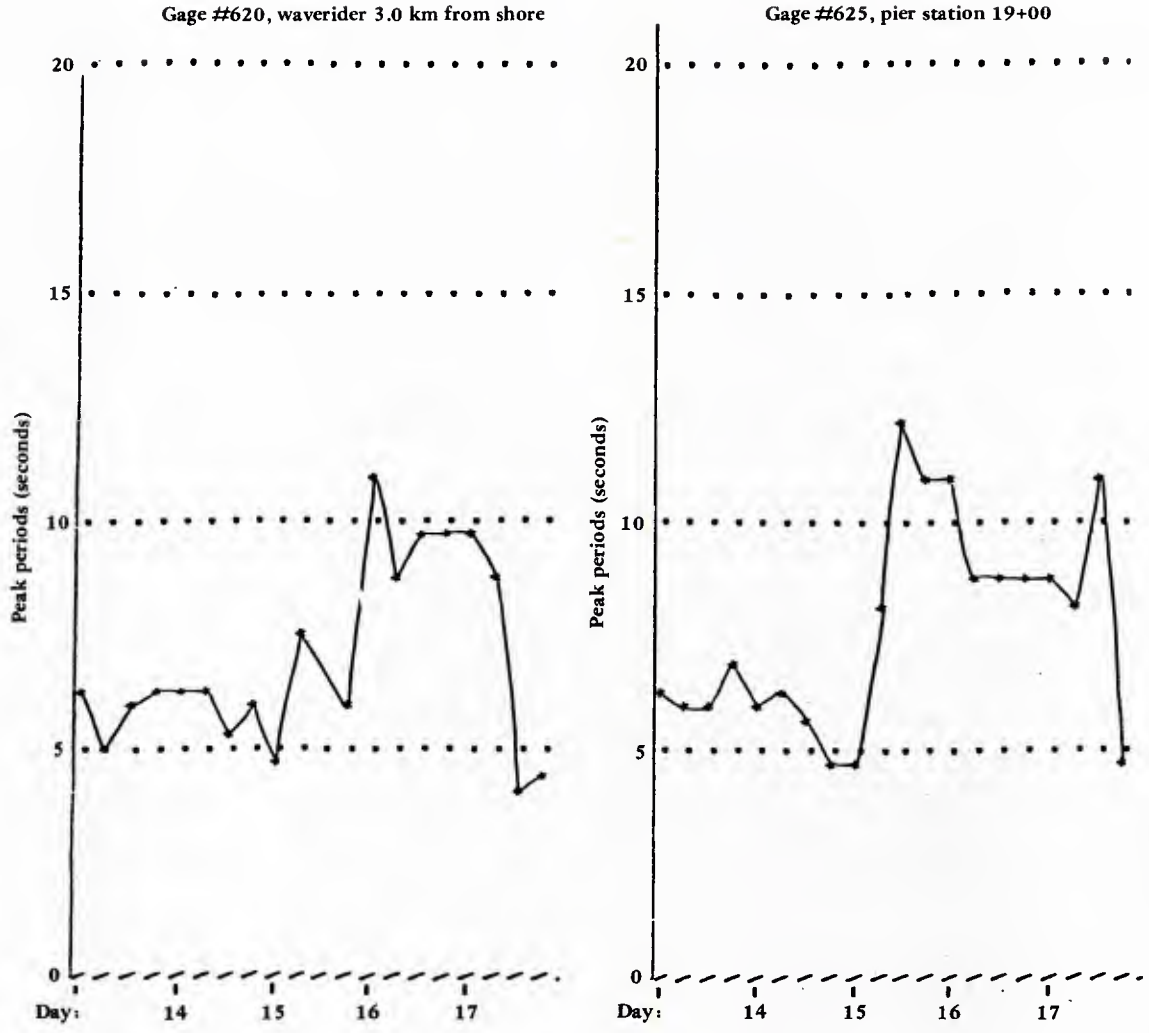

Figure B-5. Wave periods, 14 - 17 November 1983.

Appendix C

SAMPLES OF FOUR-POINT MOORING DATA

Table 3 in the main text summarized system responses and environmental excitations for each of the four-point mooring tests. However, these responses are scalar representations of complex phenomena that are functions of incident wave angle, wave frequency, and combined linear and nonlinear transfer functions. Accurate simulation of these phenomena is the true goal of a mooring model validation. The data presented here allow for isolation of many of these phenomena.

The large quantity of data collected in the Mooring Validation Experiment (MVE) four-point tests (over 600,000 data samples) is too large to include in this report. Likewise, it is also impractical to include all the analyses. The following information selected for presentation is intended to be representative:

1. Representative time series
2. Mini-Ranger displacement measurements
3. Wave excitation autospectra measured during four-point mooring tests
4. Wave buoy No. 1 and No. 2 autospectra for the same wave field
5. Representative autospectra for vessel motions and cable tensions
6. Probability density functions

The time series graphs in Figure C-1 are self-explanatory and include appropriate labels and units.

Figure C-2 shows tabular data of Mini-Ranger measurements for both the slack and taut tests. These measurements are 10-second averages, representing the position of the SEACON main mast. The two columns show east and north coordinates in the Mini-Ranger axis system.

The wave autospectra shown in Figure C-3 are plotted in feet squared-second versus bandwidth increments (multiples of 1/512 Hertz). Hamming frequency smoothing (0.25, 0.50, 0.25) was used in addition to ensemble averaging. The normalized error (e) in the autospectral ordinates is:

$$e = \sqrt{\frac{1}{nm}}$$

where: n = no. of ensembles
= 4

m = no. of averaged frequency increments
= 3

Substituting,

$$e = 0.29$$

Two distinct modal periods occur in each of the wave autospectra, and the energy between them is relatively low. This implies that the wave trains were essentially independent of each other (except for the small overlap section).

Figure C-4 has wave autospectra at each buoy for the wave field in mooring test No. 8. As expected, the spectral energy between the two buoys is virtually identical.

Figure C-5 has response autospectra for vessel motion and cable tensions. Units are feet, degrees, and pounds for the ordinates (units squared-seconds) and bandwidth increments for frequency. The normalized standard error is 0.29 as with the wave autospectra.

Figure C-6 includes probability density functions for the waves and cable tensions. The probability density functions show the actual distribution versus the equivalent Gaussian distribution (identified as *). Column information is: intervals in 12-bit integers as sampled, where 2048 is zero and each sample equals 0.0164 foot; percent of samples in each interval; and number of samples in each interval. Values in the header include number of samples (N), mean value (XBAR), and root-mean-square value (SIGMA). The waves are Gaussian as expected. The tension probabilities are decidedly non-Gaussian.

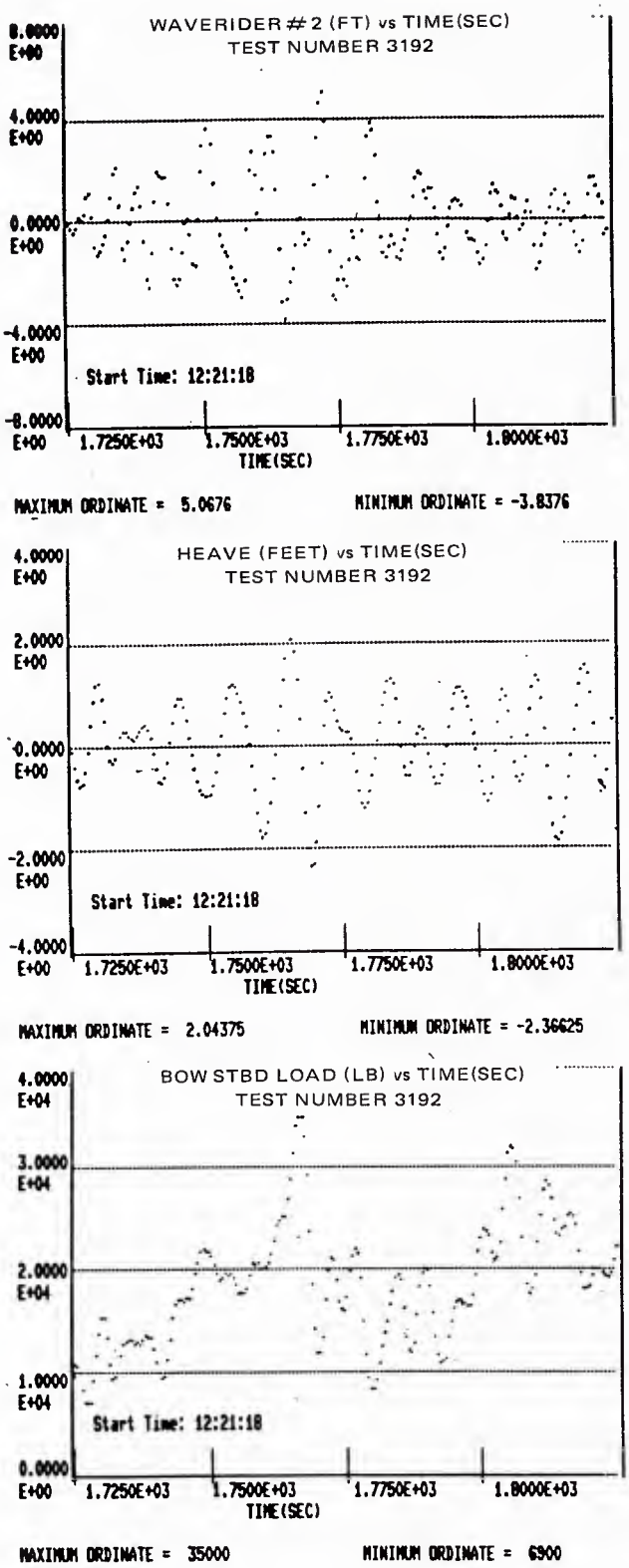

Figure C-1. Representative time series sampled data from the MVE.

Taut Moors (Tests 5-8)			Slack Moors (Tests 1-4)		
Time	X(m)	Y(m)	Time	X(m)	Y(m)
15:18:08	107	-210	11:04:01	113	-207
15:18:18	107	-207	11:04:11	114	-207
15:18:28	106	-212	11:04:21	113	-207
15:18:38	106	-211	11:04:31	113	-210
15:18:48	107	-210	11:04:41	113	-217
15:18:58	106	-208	11:04:51	113	-208
15:19:08	107	-210	11:05:01	112	-211
15:19:18	107	-207	11:05:11	112	-210
15:19:28	107	-206	11:05:21	112	-208
15:19:38	107	-207	11:05:31	113	-209
15:19:48	106	-208	11:05:41	113	-209
15:19:58	107	-208	11:05:51	114	-209
15:20:08	107	-210	11:06:01	112	-210
15:20:18	106	-209	11:06:11	113	-208
15:20:28	106	-211	11:06:21	113	-210
15:20:38	106	-211	11:06:31	113	-211
15:20:48	107	-211	11:06:41	113	-210
15:20:58	106	-209	11:06:51	113	-210
15:21:08	106	-209	11:07:01	113	-210
15:21:18	106	-209	11:07:11	112	-211
15:21:28	106	-207	11:07:21	113	-210
15:21:38	106	-210	11:07:31	114	-208
15:21:48	107	-208	11:07:41	113	-207
15:21:58	107	-210	11:07:51	113	-208
15:22:08	106	-209	11:08:01	114	-208
15:22:18	108	-208	11:08:11	113	-208
15:22:28	108	-209	11:08:21	113	-209
15:22:38	107	-211	11:08:31	112	-206
15:22:48	107	-208	11:08:41	113	-210
15:22:58	106	-208	11:08:51	113	-210
15:23:08	106	-211	11:09:01	112	-209
15:23:18	106	-212	11:09:11	112	-209
15:23:28	107	-210	11:09:21	113	-208
15:23:38	106	-207	11:09:31	113	-209
15:23:48	107	-208	11:09:41	113	-209
15:23:58	108	-209	11:09:51	113	-209
15:24:08	108	-209	11:10:01	112	-209
15:24:18	108	-209	11:10:11	112	-209
15:24:28	107	-208	11:10:21	113	-207
15:24:38	107	-210	11:10:31	113	-207
15:24:48	107	-208	11:10:41	114	-210
15:24:58	106	-209	11:10:51	114	-211
15:25:08	106	-210	11:11:01	113	-209
15:25:18	106	-208	11:11:11	113	-211
15:25:28	108	-204	11:11:21	113	-210
15:24:38	107	-211	11:11:31	112	-211
15:24:48	108	-209	11:11:41	112	-210

Notes:
(1) This Mini-Ranger coordinates, in meters, were set up such that Y is true North and X is East.
(2) The Mini-Ranger receiver was located on the SEACON main mast.

Figure C-2. Mini-Ranger vessel displacement measurements during four-point mooring tests.

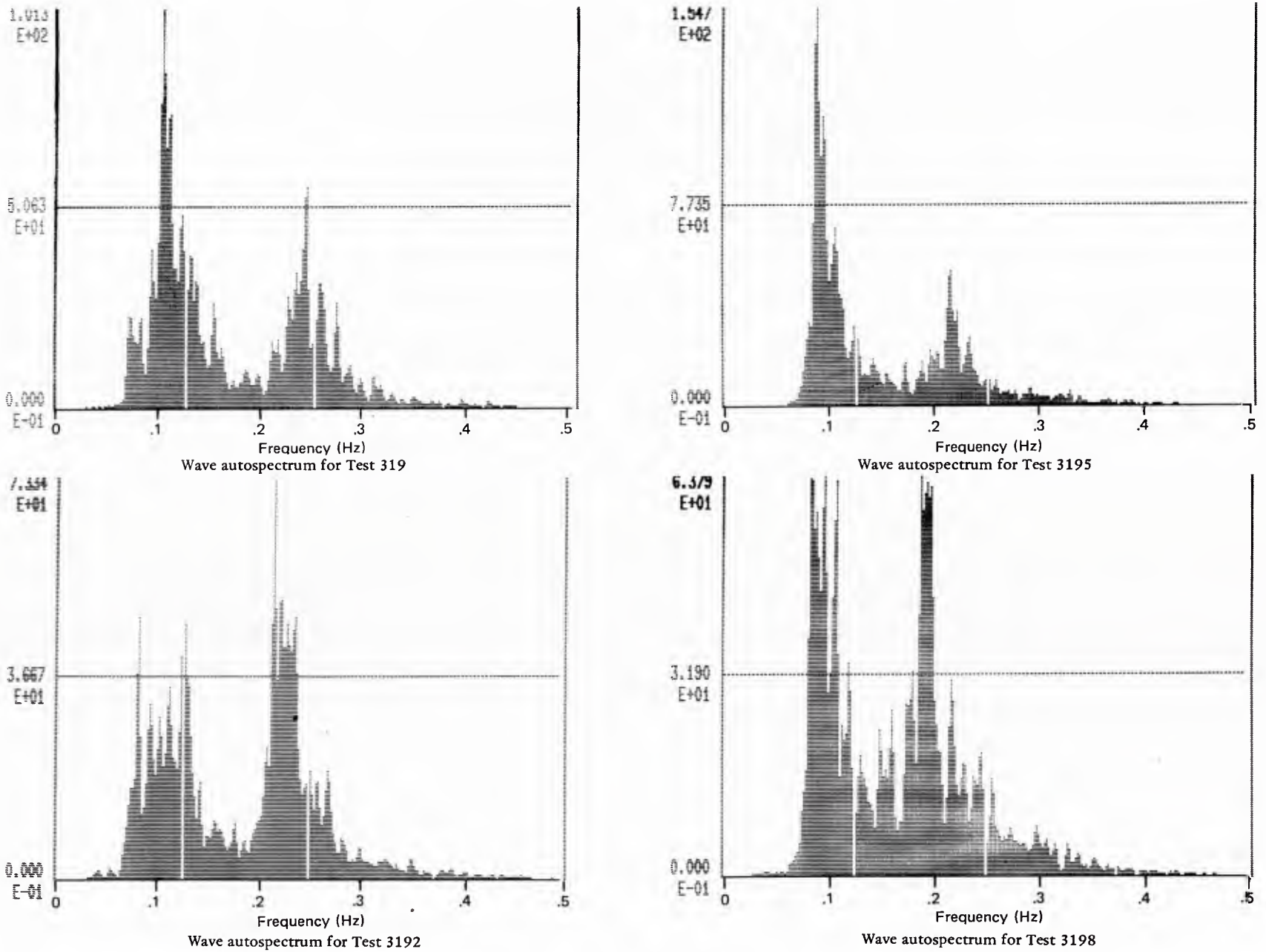

Figure C-3. Wave excitation autospectra.

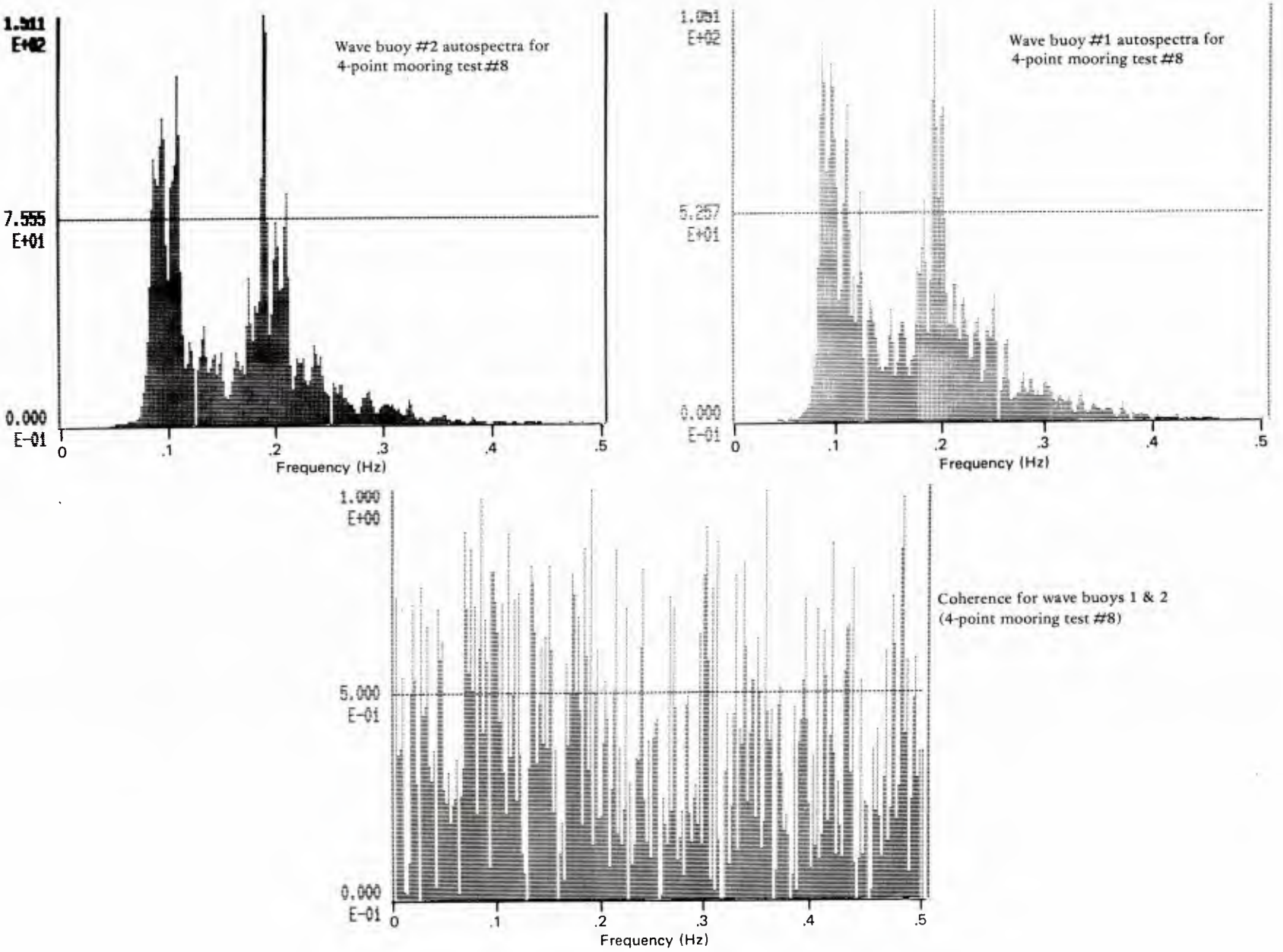

Figure C-4. Wave buoy autospectra and coherence functions.

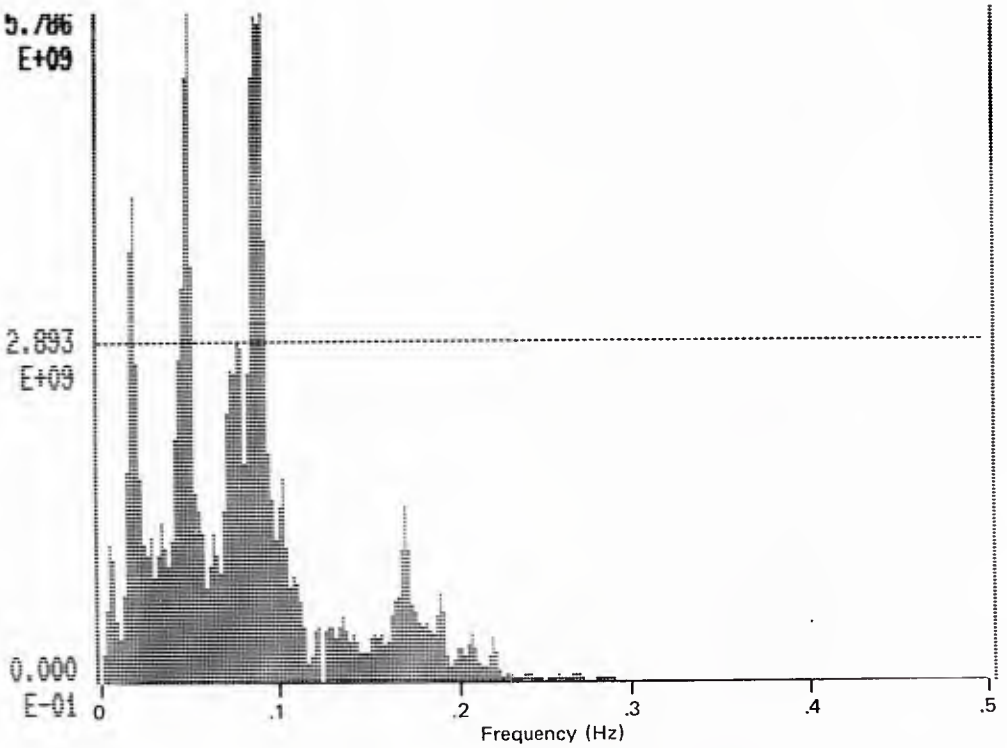

Figure C-5(a). Stern starboard tension autospectra vs frequency (four-point mooring test #5).

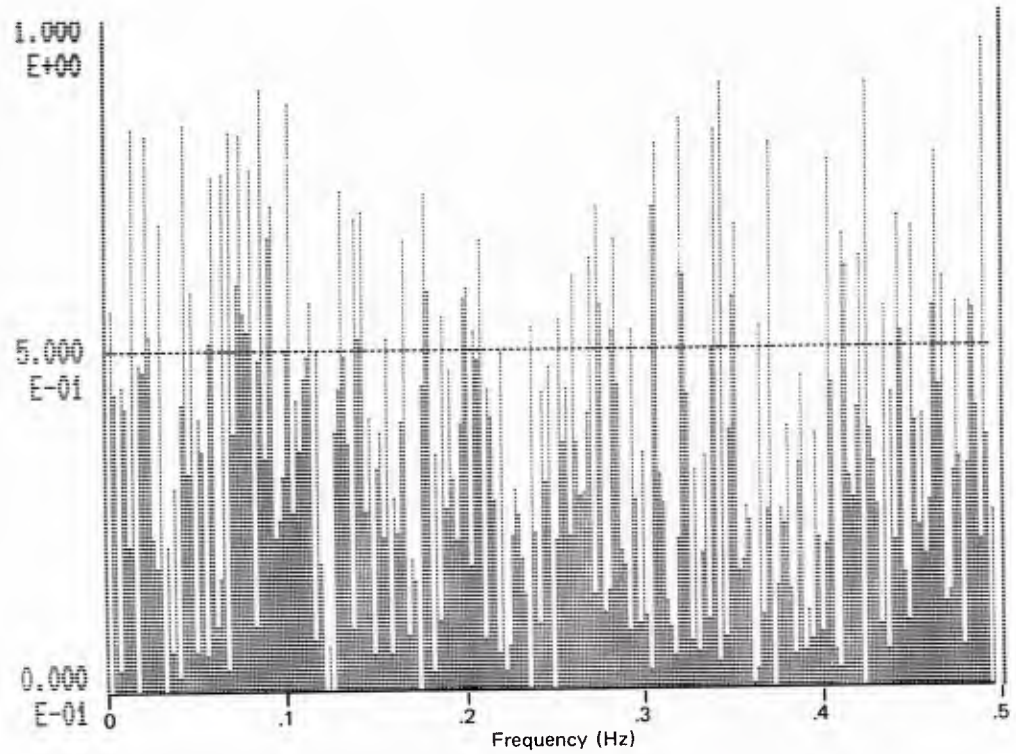

Figure C-5(a). Coherence for wave spectra and stern starboard tension (four-point mooring test #5).

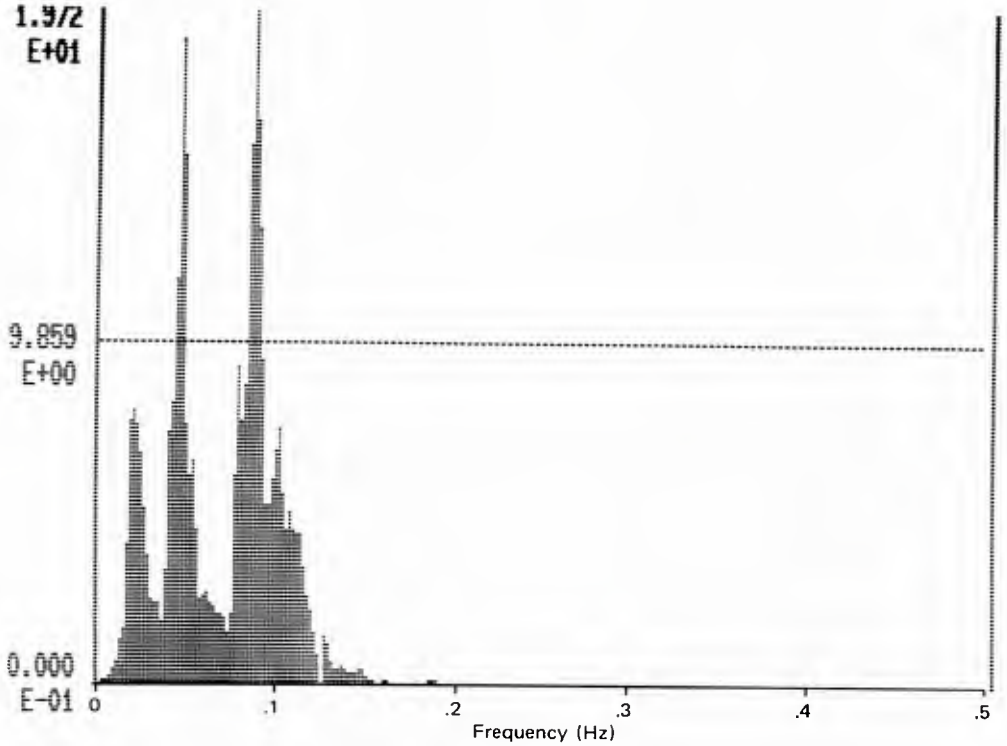

Figure C-5(b). Vessel surge autospectra vs frequency (four-point mooring test #8).

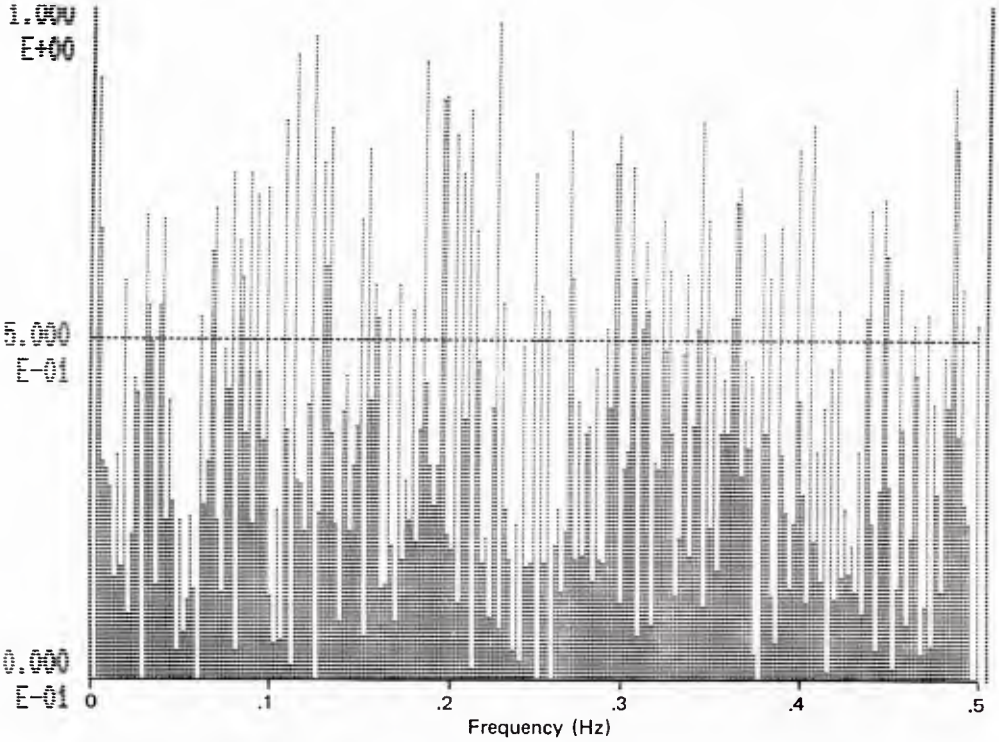

Figure C-5(b). Coherence for vessel surge vs wave spectra (four-point mooring test #8).

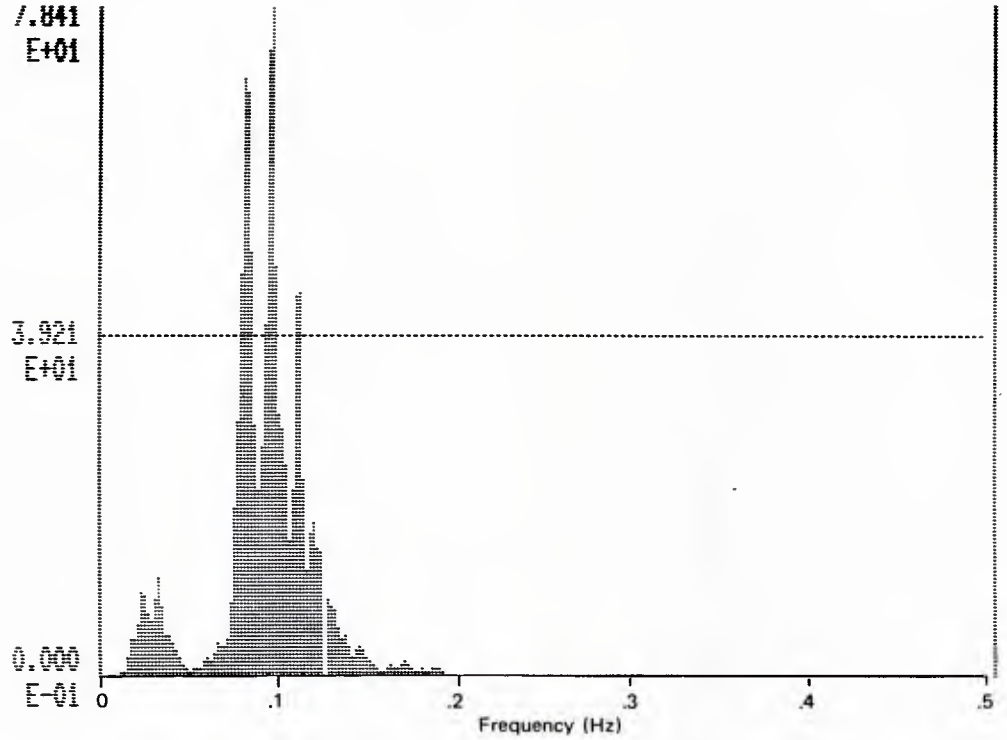

Figure C-5(c). Vessel sway autospectra vs frequency (four-point mooring test #8).

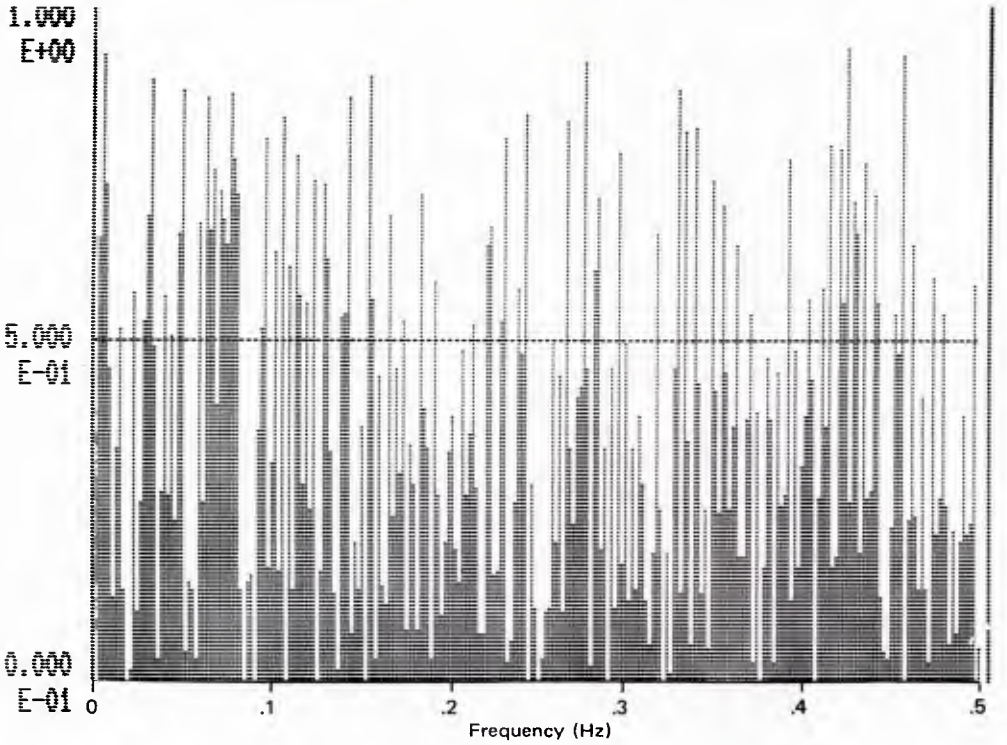

Figure C-5(c). Coherence for wave spectra and vessel sway (four-point mooring test #8).

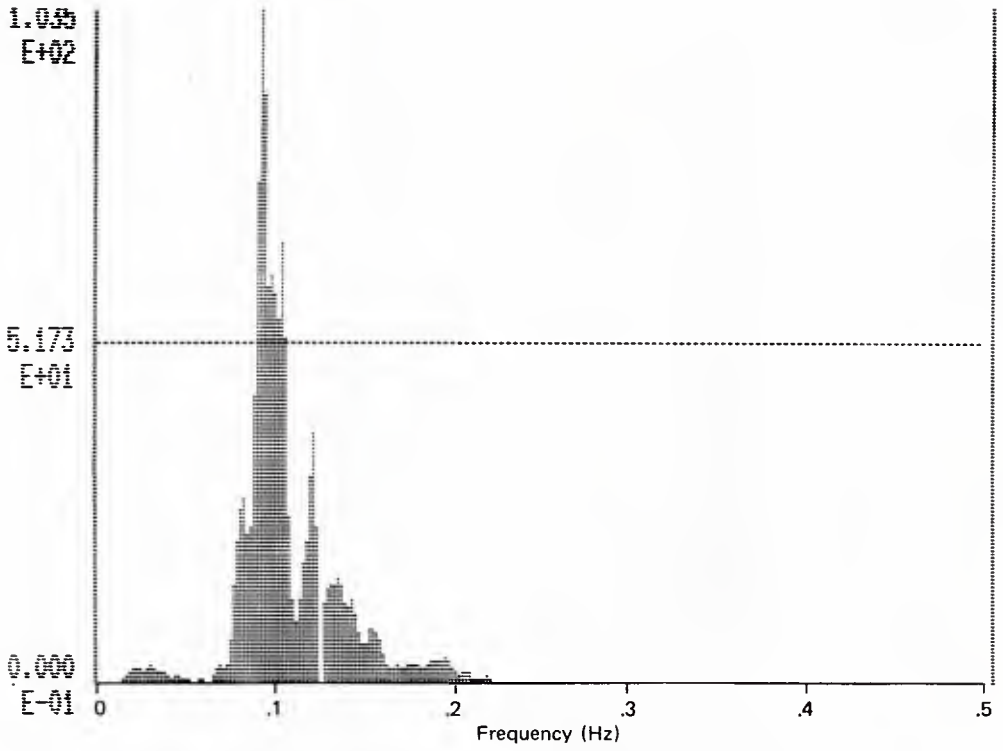

Figure C-5(d). Vessel heave autospectra vs frequency (four-point mooring test #5).

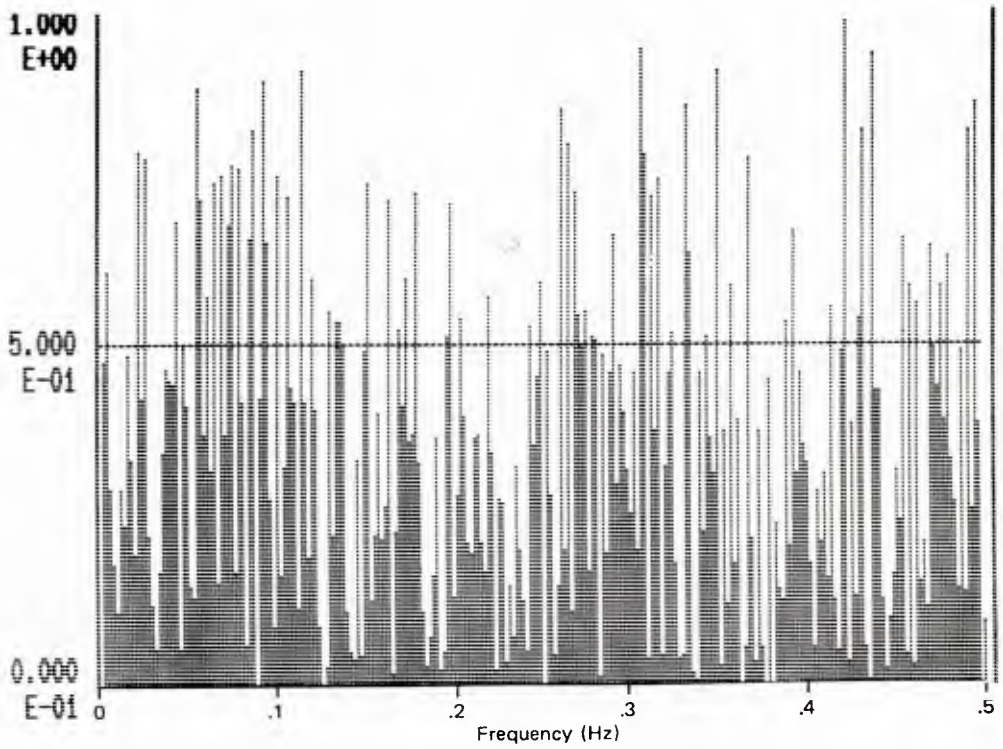

Figure C-5(d). Coherence for vessel heave and wave spectra (four-point mooring test #5).

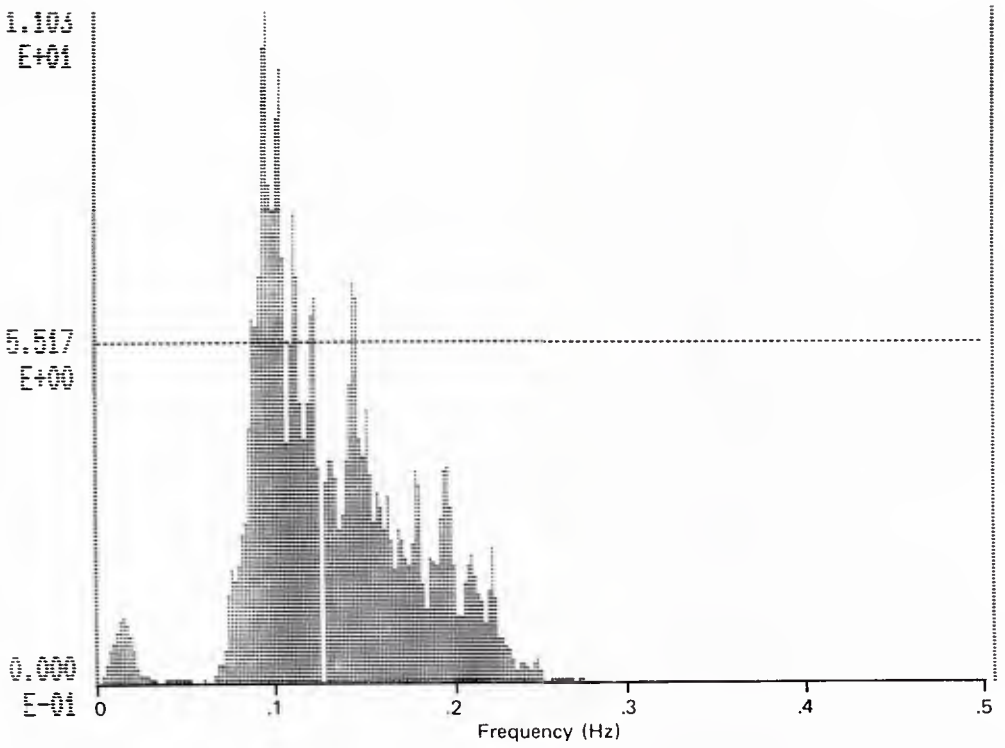

Figure C-5(e). Coherence for vessel pitch and wave spectra (four-point mooring test #5).

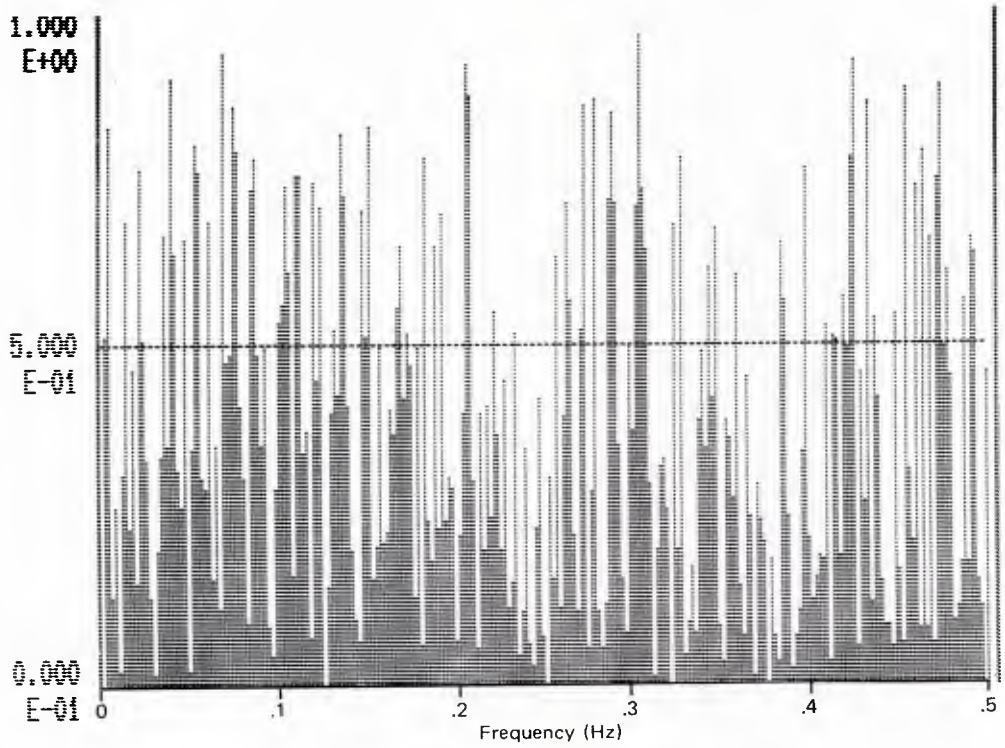

Figure C-5(e). Vessel pitch autospectra vs frequency (four-point mooring test #5).

```
          PROCESSING FOR FILENAME=DY1:MSPCHN.026
 N  =   4034 XBAR    = 2044.82 SIGMA=   82.27 SE=    1.30

      HISTOGRAM FOR TEST 3195 WITH AN INTERVAL OF   20

INTERVAL    %      #  0
1681-1700   0      0->     .   .   .   .   .   .   .   .   .   .   .   .   .   .   .   .   .   .   .   .   .   .
1701-1720   0      0->     .   .   .   .   .   .   .   .   .   .   .   .   .   .   .   .   .   .   .   .   .   .
1721-1740   0      0->     .   .   .   .   .   .   .   .   .   .   .   .   .   .   .   .   .   .   .   .   .   .
1741-1760   0      0->     .   .   .   .   .   .   .   .   .   .   .   .   .   .   .   .   .   .   .   .   .   .
1761-1780   0      1->     .   .   .   .   .   .   .   .   .   .   .   .   .   .   .   .   .   .   .   .   .   .
1781-1800   0      3-> #   .   .   .   .   .   .   .   .   .   .   .   .   .   .   .   .   .   .   .   .   .   .
1801-1820   0      9-> #   .   .   .   .   .   .   .   .   .   .   .   .   .   .   .   .   .   .   .   .   .   .
1821-1840   0     17-> #   .   .   .   .   .   .   .   .   .   .   .   .   .   .   .   .   .   .   .   .   .   .
1841-1860   1     30-> ===#,  .   .   .   .   .   .   .   .   .   .   .   .   .   .   .   .   .   .   .   .   .
1861-1880   1     45-> ====, #  .   .   .   .   .   .   .   .   .   .   .   .   .   .   .   .   .   .   .   .   .
1881-1900   2    100-> ====,=== #   .   .   .   .   .   .   .   .   .   .   .   .   .   .   .   .   .   .   .   .
1901-1920   4    143-> ====,====,====#=   .   .   .   .   .   .   .   .   .   .   .   .   .   .   .   .   .   .
1921-1940   5    196-> ====,====,====,====,#   .   .   .   .   .   .   .   .   .   .   .   .   .   .   .   .   .
1941-1960   5    219-> ====,====,====,====,=   ,#  .   .   .   .   .   .   .   .   .   .   .   .   .   .   .   .
1961-1980   6    249-> ====,====,====,====,====,     . #  .   .   .   .   .   .   .   .   .   .   .   .   .   .
1981-2000   8    327-> ====,====,====,====,====,====,=== ,#   .   .   .   .   .   .   .   .   .   .   .   .   .
2001-2020   9    354-> ====,====,====,====,====,====,====,== #,  .   .   .   .   .   .   .   .   .   .   .   .
2021-2040   9    373-> ====,====,====,====,====,====,====,==  #  .   .   .   .   .   .   .   .   .   .   .   .
2041-2060  10    408-> ====,====,====,====,====,====,====,==#=,=  .   .   .   .   .   .   .   .   .   .   .   .
2061-2080   9    374-> ====,====,====,====,====,====,===#,==  .   .   .   .   .   .   .   .   .   .   .   .   .
2081-2100   7    301-> ====,====,====,====,====,===#,   .   .   .   .   .   .   .   .   .   .   .   .   .   .
2101-2120   7    278-> ====,====,====,====,==#=,====,   .   .   .   .   .   .   .   .   .   .   .   .   .   .
2121-2140   5    206-> ====,====,====,==#=,=   .   .   .   .   .   .   .   .   .   .   .   .   .   .   .   .
2141-2160   4    147-> ====,====,==#=,=   .   .   .   .   .   .   .   .   .   .   .   .   .   .   .   .   .   .
2161-2180   3    101-> ====,==#=,==   .   .   .   .   .   .   .   .   .   .   .   .   .   .   .   .   .   .   .
2181-2200   2     73-> ====#===  .   .   .   .   .   .   .   .   .   .   .   .   .   .   .   .   .   .   .   .
2201-2220   1     33-> ==#=,    .   .   .   .   .   .   .   .   .   .   .   .   .   .   .   .   .   .   .   .
2221-2240   0     20-> #  .   .   .   .   .   .   .   .   .   .   .   .   .   .   .   .   .   .   .   .   .   .
2241-2260   0     12-> #  .   .   .   .   .   .   .   .   .   .   .   .   .   .   .   .   .   .   .   .   .   .
2261-2280   0      8->     .   .   .   .   .   .   .   .   .   .   .   .   .   .   .   .   .   .   .   .   .   .
2281-2300   0      3->     .   .   .   .   .   .   .   .   .   .   .   .   .   .   .   .   .   .   .   .   .   .
2301-2320   0      1->     .   .   .   .   .   .   .   .   .   .   .   .   .   .   .   .   .   .   .   .   .   .
2321-2340   0      2->     .   .   .   .   .   .   .   .   .   .   .   .   .   .   .   .   .   .   .   .   .   .
2341-2360   0      0->     .   .   .   .   .   .   .   .   .   .   .   .   .   .   .   .   .   .   .   .   .   .

          PROCESSING FOR FILENAME=DY1:MSPCHN.027
 N  =   4034 XBAR    = 2045.58 SIGMA=   83.40 SE=    1.31

      HISTOGRAM FOR TEST 3195 WITH AN INTERVAL OF   20

INTERVAL    %      #  0
1681-1700   0      0->     .   .   .   .   .   .   .   .   .   .   .   .   .   .   .   .   .   .   .   .   .   .
1701-1720   0      0->     .   .   .   .   .   .   .   .   .   .   .   .   .   .   .   .   .   .   .   .   .   .
1721-1740   0      0->     .   .   .   .   .   .   .   .   .   .   .   .   .   .   .   .   .   .   .   .   .   .
1741-1760   0      0->     .   .   .   .   .   .   .   .   .   .   .   .   .   .   .   .   .   .   .   .   .   .
1761-1780   0      1->     .   .   .   .   .   .   .   .   .   .   .   .   .   .   .   .   .   .   .   .   .   .
1781-1800   0      2-> #   .   .   .   .   .   .   .   .   .   .   .   .   .   .   .   .   .   .   .   .   .   .
1801-1820   0      8-> #   .   .   .   .   .   .   .   .   .   .   .   .   .   .   .   .   .   .   .   .   .   .
1821-1840   0     20->  #  .   .   .   .   .   .   .   .   .   .   .   .   .   .   .   .   .   .   .   .   .   .
1841-1860   1     39-> ===#,  .   .   .   .   .   .   .   .   .   .   .   .   .   .   .   .   .   .   .   .   .
1861-1880   2     62-> ====,=#= .   .   .   .   .   .   .   .   .   .   .   .   .   .   .   .   .   .   .   .   .
1881-1900   2     87-> ====,===  ,#   .   .   .   .   .   .   .   .   .   .   .   .   .   .   .   .   .   .   .
1901-1920   3    119-> ====,====,=== #   .   .   .   .   .   .   .   .   .   .   .   .   .   .   .   .   .   .
1921-1940   4    162-> ====,====,====,==  ,#  .   .   .   .   .   .   .   .   .   .   .   .   .   .   .   .   .
1941-1960   5    219-> ====,====,====,====,=   ,#  .   .   .   .   .   .   .   .   .   .   .   .   .   .   .   .
1961-1980   6    254-> ====,====,====,====,====,     . #  .   .   .   .   .   .   .   .   .   .   .   .   .   .
1981-2000   9    349-> ====,====,====,====,====,====,====,====,#== .   .   .   .   .   .   .   .   .   .   .   .
2001-2020  10    385-> ====,====,====,====,====,====,====,====,===#,==  .   .   .   .   .   .   .   .   .   .   .
2021-2040  10    417-> ====,====,====,====,====,====,====,====,====#==  .   .   .   .   .   .   .   .   .   .   .
2041-2060   9    376-> ====,====,====,====,====,====,====,====,==# .   .   .   .   .   .   .   .   .   .   .   .
2061-2080   9    354-> ====,====,====,====,====,====,====,====#=== .   .   .   .   .   .   .   .   .   .   .   .
2081-2100   8    309-> ====,====,====,====,====,====,====#===  .   .   .   .   .   .   .   .   .   .   .   .   .
2101-2120   6    234-> ====,====,====,====,====,===#,  .   .   .   .   .   .   .   .   .   .   .   .   .   .   .
2121-2140   5    194-> ====,====,====,==#=,=   .   .   .   .   .   .   .   .   .   .   .   .   .   .   .   .   .
2141-2160   4    166-> ====,====,==#=,==   .   .   .   .   .   .   .   .   .   .   .   .   .   .   .   .   .   .
2161-2180   2    100-> ====,===#,   .   .   .   .   .   .   .   .   .   .   .   .   .   .   .   .   .   .   .   .
2181-2200   2     63-> ====,#== .   .   .   .   .   .   .   .   .   .   .   .   .   .   .   .   .   .   .   .   .
2201-2220   1     50-> ==#=,    .   .   .   .   .   .   .   .   .   .   .   .   .   .   .   .   .   .   .   .   .
2221-2240   1     34-> =#==,    .   .   .   .   .   .   .   .   .   .   .   .   .   .   .   .   .   .   .   .   .
2241-2260   0     15-> #  .   .   .   .   .   .   .   .   .   .   .   .   .   .   .   .   .   .   .   .   .   .
2261-2280   0      8-> #  .   .   .   .   .   .   .   .   .   .   .   .   .   .   .   .   .   .   .   .   .   .
2281-2300   0      4->     .   .   .   .   .   .   .   .   .   .   .   .   .   .   .   .   .   .   .   .   .   .
2301-2320   0      1->     .   .   .   .   .   .   .   .   .   .   .   .   .   .   .   .   .   .   .   .   .   .
2321-2340   0      2->     .   .   .   .   .   .   .   .   .   .   .   .   .   .   .   .   .   .   .   .   .   .
2341-2360   0      0->     .   .   .   .   .   .   .   .   .   .   .   .   .   .   .   .   .   .   .   .   .   .
```

Figure C-6(a). Wave probability density function (four-point mooring test #5).

PROCESSING FOR FILENAME=DY1:MSPCHN.001

N = 4034 XBAR = 2230.40 SIGMA= 40.55 SE= 0.64

HISTOGRAM FOR TEST 3195 WITH AN INTERVAL OF 15

INTERVAL	%	#
2041-2055	0	0
2056-2070	0	0
2071-2085	0	0
2086-2100	0	0
2101-2115	0	4
2116-2130	1	27
2131-2145	1	49
2146-2160	2	83
2161-2175	5	193
2176-2190	9	382
2191-2205	14	577
2206-2220	18	740
2221-2235	16	648
2236-2250	12	464
2251-2265	8	337
2266-2280	5	192
2281-2295	4	148
2296-2310	2	68
2311-2325	1	51
2326-2340	1	26
2341-2355	0	17
2356-2370	0	14
2371-2385	0	10

PROCESSING FOR FILENAME=DY1:MSPCHN.004

N = 4034 XBAR = 2167.66 SIGMA= 47.25 SE= 0.74

HISTOGRAM FOR TEST 3195 WITH AN INTERVAL OF 15

INTERVAL	%	#
1951-1965	0	0
1966-1980	0	0
1981-1995	0	0
1996-2010	0	0
2011-2025	0	0
2026-2040	0	0
2041-2055	0	0
2056-2070	0	7
2071-2085	1	45
2086-2100	3	117
2101-2115	8	328
2116-2130	13	522
2131-2145	17	700
2146-2160	15	598
2161-2175	14	554
2176-2190	9	381
2191-2205	6	238
2206-2220	4	177
2221-2235	2	89
2236-2250	2	80
2251-2265	1	53
2266-2280	1	48
2281-2295	1	26
2296-2310	0	16
2311-2325	0	15
2326-2340	0	14
2341-2355	0	7

PROCESSING FOR FILENAME=DY1:MSPCHN.007

N = 4034 XBAR = 2125.52 SIGMA= 75.01 SE= 1.18

HISTOGRAM FOR TEST 3195 WITH AN INTERVAL OF 15

INTERVAL	%	#
1801-1815	0	0
1816-1830	0	0
1831-1845	0	0
1846-1860	0	0
1861-1875	0	0
1876-1890	0	0
1891-1905	0	0
1906-1920	0	0
1921-1935	0	0
1936-1950	0	0
1951-1965	0	0
1966-1980	0	0
1981-1995	0	0
1996-2010	0	0
2011-2025	0	0
2026-2040	0	16
2041-2055	5	195
2056-2070	22	879
2071-2085	18	744
2086-2100	13	507
2101-2115	8	333
2116-2130	6	226
2131-2145	5	192
2146-2160	4	147
2161-2175	3	127
2176-2190	2	87
2191-2205	2	96
2206-2220	2	70
2221-2235	2	61
2236-2250	1	48
2251-2265	1	44
2266-2280	1	46
2281-2295	1	38
2296-2310	1	29
2311-2325	1	33
2326-2340	1	23
2341-2355	0	20
2356-2370	0	14
2371-2385	0	15
2386-2400	0	9
2401-2415	0	9

PROCESSING FOR FILENAME=DY1:MSPCHN.010

N = 4034 XBAR = 2212.41 SIGMA= 121.45 SE= 1.91

HISTOGRAM FOR TEST 3195 WITH AN INTERVAL OF 30

INTERVAL	%	#
1681-1710	0	0
1711-1740	0	0
1741-1770	0	0
1771-1800	0	0
1801-1830	0	0
1831-1860	0	0
1861-1890	0	0
1891-1920	0	0
1921-1950	0	0
1951-1980	0	0
1981-2010	0	0
2011-2040	0	10
2041-2070	5	215
2071-2100	18	741
2101-2130	14	577
2131-2160	10	392
2161-2190	10	406
2191-2220	8	323
2221-2250	6	252
2251-2280	6	227
2281-2310	4	174
2311-2340	4	167
2341-2370	4	142
2371-2400	3	110
2401-2430	2	75
2431-2460	2	72
2461-2490	1	43
2491-2520	1	26
2521-2550	1	25
2551-2580	1	23
2581-2610	0	14
2611-2640	0	4
2641-2670	0	1

Figure C-6(b). Cable tension probability density functions.

DISTRIBUTION LIST

NATL ACADEMY OF ENGRG Alexandria, VA
ARMY BELVOIR R&D CEN STRBE-WC, Ft Belvoir, VA
ARMY EWES Library, Vicksburg MS
CNO Code OP 23, Washington, DC; Code OP 323, Washington DC
COGARD R AND DC Library, Groton, CT
COMDT COGARD Library, Washington, DC
COMSC Washington DC
DTIC Alexandria, VA
DTNSRDC Code 1541 (Rispin), Bethesda, MD; DET, Code 522 (Library), Annapolis, MD
LIBRARY OF CONGRESS Sci & Tech Div, Washington, DC
NATL RESEARCH COUNCIL Naval Studies Bd, Washington, DC; Naval Studies Board, Washington, DC
NAVCOASTSYSCEN Tech Library, Panama City, FL
NAVFACENGCOM Code 03, Alexandria, VA; Code 03T (Essoglou), Alexandria, VA; Code 07A (Herrmann), Alexandria, VA; Code 09M124 (Lib), Alexandria, VA; Code FPO-3C, Alexandria, VA
NAVFACENGCOM - CHES DIV. Code 407 (D Scheesele) Washington, DC; Code FPO-1E, Washington, DC; Code FPO-1PL, Washington, DC
NAVFACENGCOM - LANT DIV. Library, Norfolk, VA
NAVFACENGCOM - NORTH DIV. Code 04AL, Philadelphia, PA
NAVFACENGCOM - PAC DIV. Library, Pearl Harbor, HI
NAVFACENGCOM - SOUTH DIV. Library, Charleston, SC
NAVFACENGCOM - WEST DIV. Library (Code 04A2.2), San Bruno, CA
NAVFACENGCOM CONTRACTS ROICC, Beaufort, SC
NAVOCEANSYSCEN Code 94 (Talkington), San Diego, CA; Code 964 (Tech Library), San Diego, CA; Code 9642B (Bayside Library), San Diego, CA; DET, R Yumori, Kailua, HI; DET, Tech Lib, Kailua, HI
NAVPGSCOL Code 1424, Library, Monterey, CA
NAVSHIPYD Code 202.4, Long Beach, CA; Code 440, Portsmouth, NH; Library, Portsmouth, NH
NORDA Ocean Rsch Off (Code 440), Bay St. Louis, MS
NRL Code 5800, Washington, DC; Ocean Tech Div (O. Griffith), Washington, DC
CNR DET, Dir, Boston, MA; DET, Dir, Pasadena, CA
PWC Code 101 (Library), Oakland, CA; Code 123-C, San Diego, CA; Code 420, Great Lakes, IL; Library (Code 134), Pearl Harbor, HI; Library, Guam, Mariana Islands; Library, Norfolk, VA; Library, Pensacola, FL; Library, Yokosuka JA; Tech Library, Subic Bay, RP
U.S. MERCHANT MARINE ACADEMY Reprint Custodian, Kings Point, NY
USNA Chairman, Mech Engrg Dept, Annapolis, MD
ADVANCED TECHNOLOGY Ops Cen Mgr (Moss), Camarillo, CA
COLORADO SCHOOL OF MINES Dept of Engrg (Chung), Golden, CO
DUKE UNIV CE Dept (Muga), Durham, NC
FLORIDA ATLANTIC UNIVERSITY Ocean Engrg Dept (McAllister), Boca Raton, FL; Ocean Engrg Dept (Su), Boca Raton, FL
JOHNS HOPKINS UNIV CE Dept (Jones), Baltimore, MD
MAINE MARITIME ACADEMY Lib, Castine, ME
MIT Lib, Tech Reports, Cambridge, MA; Ocean Engrg Dept (Vandiver), Cambridge, MA
OREGON STATE UNIVERSITY CE Dept (Grace), Corvallis, OR
PURDUE UNIVERSITY CE Scol (Altschaeffl), Lafayette, IN
TEXAS A&M UNIVERSITY CE Dept (Niedzwecki), College Station, TX; Ocean Engr Proj, College Station, TX
UNIVERSITY OF CALIFORNIA CE Dept (Gerwick), Berkeley, CA; Naval Arch Dept, Berkeley, CA
UNIVERSITY OF DELAWARE CE Dept, Ocean Engrg (Dalrymple), Newark, DE
UNIVERSITY OF HAWAII Ocean Engrg Dept (Ertekin), Honolulu, HI
UNIVERSITY OF MICHIGAN CE Dept (Richart), Ann Arbor, MI
UNIVERSITY OF RHODE ISLAND CE Dept (Kovacs), Kingston, RI
UNIVERSITY OF WASHINGTON CE Dept, Seattle, WA
WOODS HOLE OCENAOGRAPHIC INST Doc Lib, Woods Hole, MA
AMETEK OFFSHORE RSCH Santa Barbara, CA
ATLANTIC RICHFIELD CO RE Smith, Dallas, TX
BROWN & ROOT Ward, Houston, TX
CANADA Viateur De Champlain, D.S.A., Matane, Canada
COLUMBIA GULF TRANSMISSION CO. Engrg Lib, Houston, TX
CONTINENTAL OIL CO O. Maxson, Ponca City, OK
DRAVO CORP Wright, Pittsburg, PA
EASTPORT INTL, INC Mgr (JH Osborn), Ventura, CA
EG&G WASH ANAL SVC CEN, INC Bonde, Rockville, MD
EVALUATION ASSOC. INC MA Fedele, King of Prussia, PA

GIANNOTTI & ASSOC, INC Annapolis, MD
HALEY & ALDRICH, INC. HP Aldrich, Jr, Cambridge, MA
JOHN J MCMULLEN ASSOC Library, New York, NY
LIN OFFSHORE ENGRG P. Chow, San Francisco CA
MARATHON OIL CO Houston TX
MOBIL R & D CORP Offshore Eng Library, Dallas, TX
MOFFATT & NICHOL ENGRS R Palmer, Long Beach, CA
PACIFIC MARINE TECHNOLOGY (M. Wagner) Duvall, WA
R J BROWN ASSOC R Perera, Houston, TX
SCHUPACK SUAREZ ENGRS, INC M. Schupack, Norwalk, CT
SHELL OFFSHORE INC E Doyle, Houston, TX
SHELL OIL CO E&P Civil Engrg, Houston, TX
WESTERN INSTRUMENT CORP Ventura, CA
WESTINGHOUSE ELECTRIC CORP. Oceanic Div Lib, Annapolis, MD
WOODWARD-CLYDE CONSULTANTS W Reg, Lib, Walnut Creek, CA
MARINE RESOURCES DEV FOUNDATION N.T. Monney, Annapolis, MD

DISTRIBUTION QUESTIONNAIRE

The Naval Civil Engineering Laboratory is revising its primary distribution lists.

SUBJECT CATEGORIES

1 SHORE FACILITIES
2 Construction methods and materials (including corrosion control, coatings)
3 Waterfront structures (maintenance/deterioration control)
4 Utilities (including power conditioning)
5 Explosives safety
6 Construction equipment and machinery
7 Fire prevention and control
8 Antenna technology
9 Structural analysis and design (including numerical and computer techniques)
10 Protective construction (including hardened shelters, shock and vibration studies)
11 Soil/rock mechanics
13 BEQ
14 Airfields and pavements
15 ADVANCED BASE AND AMPHIBIOUS FACILITIES
16 Base facilities (including shelters, power generation, water supplies)
17 Expedient roads/airfields/bridges
18 Amphibious operations (including breakwaters, wave forces)
19 Over-the-Beach operations (including containerization, materiel transfer, lighterage and cranes)
20 POL storage, transfer and distribution
24 POLAR ENGINEERING
24 Same as Advanced Base and Amphibious Facilities, except limited to cold-region environments
28 ENERGY/POWER GENERATION
29 Thermal conservation (thermal engineering of buildings, HVAC systems, energy loss measurement, power generation)
30 Controls and electrical conservation (electrical systems, energy monitoring and control systems)
31 Fuel flexibility (liquid fuels, coal utilization, energy from solid waste)
32 Alternate energy source (geothermal power, photovoltaic power systems, solar systems, wind systems, energy storage systems)
33 Site data and systems integration (energy resource data, energy consumption data, integrating energy systems)
34 ENVIRONMENTAL PROTECTION
35 Solid waste management
36 Hazardous/toxic materials management
37 Wastewater management and sanitary engineering
38 Oil pollution removal and recovery
39 Air pollution
40 Noise abatement
44 OCEAN ENGINEERING
45 Seafloor soils and foundations
46 Seafloor construction systems and operations (including diver and manipulator tools)
47 Undersea structures and materials
48 Anchors and moorings
49 Undersea power systems, electromechanical cables, and connectors
50 Pressure vessel facilities
51 Physical environment (including site surveying)
52 Ocean-based concrete structures
53 Hyperbaric chambers
54 Undersea cable dynamics

TYPES OF DOCUMENTS

85 Techdata Sheets **86 Technical Reports and Technical Notes** **82 NCEL Guide & Updates** ☐ **None— remove my name**

83 Table of Contents & Index to TDS **91 Physical Security**

INSTRUCTIONS

The Naval Civil Engineering Laboratory has revised its primary distribution lists. The bottom of the mailing label has several numbers listed. These numbers correspond to numbers assigned to the list of Subject Categories. Numbers on the label corresponding to those on the list indicate the subject category and type of documents you are presently receiving. If you are satisfied, throw this card away (or file it for later reference).

If you want to change what you are presently receiving:

- Delete – mark off number on bottom of label.
- Add – circle number on list.
- Remove my name from all your lists – check box on list.
- Change my address – line out incorrect line and write in correction (ATTACH MAILING LABEL).
- Number of copies should be entered after the title of the subject categories you select.

Fold on line below and drop in the mail.

Note: Numbers on label but not listed on questionnaire are for NCEL use only, please ignore them.

Fold on line and staple.

DEPARTMENT OF THE NAVY

NAVAL CIVIL ENGINEERING LABORATORY
PORT HUENEME, CALIFORNIA 93043

OFFICIAL BUSINESS
PENALTY FOR PRIVATE USE, $300
1 IND-NCEL-2700/4 (REV. 12-73)
0930-LL-L70-0044

POSTAGE AND FEES PAID
DEPARTMENT OF THE NAVY
DOD-316

Commanding Officer
Code L14
Naval Civil Engineering Laboratory
Port Hueneme, California 93043

DISTRIBUTION QUESTIONNAIRE

The Naval Civil Engineering Laboratory is revising its primary distribution lists.

SUBJECT CATEGORIES

1 **SHORE FACILITIES**
2 Construction methods and materials (including corrosion control, coatings)
3 Waterfront structures (maintenance/deterioration control)
4 Utilities (including power conditioning)
5 Explosives safety
6 Construction equipment and machinery
7 Fire prevention and control
8 Antenna technology
9 Structural analysis and design (including numerical and computer techniques)
10 Protective construction (including hardened shelters, shock and vibration studies)
11 Soil/rock mechanics
13 BEQ
14 Airfields and pavements
15 ADVANCED BASE AND AMPHIBIOUS FACILITIES
16 Base facilities (including shelters, power generation, water supplies)
17 Expedient roads/airfields/bridges
18 Amphibious operations (including breakwaters, wave forces)
19 Over-the-Beach operations (including containerization, materiel transfer, lighterage and cranes)
20 POL storage, transfer and distribution
24 POLAR ENGINEERING
24 Same as Advanced Base and Amphibious Facilities, except limited to cold-region environments
28 ENERGY/POWER GENERATION
29 Thermal conservation (thermal engineering of buildings, HVAC systems, energy loss measurement, power generation)
30 Controls and electrical conservation (electrical systems, energy monitoring and control systems)
31 Fuel flexibility (liquid fuels, coal utilization, energy from solid waste)
32 Alternate energy source (geothermal power, photovoltaic power systems, solar systems, wind systems, energy storage systems)
33 Site data and systems integration (energy resource data, energy consumption data, integrating energy systems)
34 ENVIRONMENTAL PROTECTION
35 Solid waste management
36 Hazardous/toxic materials management
37 Wastewater management and sanitary engineering
38 Oil pollution removal and recovery
39 Air pollution
40 Noise abatement
44 OCEAN ENGINEERING
45 Seafloor soils and foundations
46 Seafloor construction systems and operations (including diver and manipulator tools)
47 Undersea structures and materials
48 Anchors and moorings
49 Undersea power systems, electromechanical cables, and connectors
50 Pressure vessel facilities
51 Physical environment (including site surveying)
52 Ocean-based concrete structures
53 Hyperbaric chambers
54 Undersea cable dynamics

TYPES OF DOCUMENTS

85 Techdata Sheets **86 Technical Reports and Technical Notes** **82 NCEL Guide & Updates** ☐ None—remove my name

83 Table of Contents & Index to TDS **91 Physical Security**

PLEASE HELP US PUT THE ZIP IN YOUR MAIL! ADD YOUR FOUR NEW ZIP DIGITS TO YOUR LABEL (OR FACSIMILE), STAPLE INSIDE THIS SELF-MAILER, AND RETURN TO US.

(fold here)

DEPARTMENT OF THE NAVY

NAVAL CIVIL ENGINEERING LABORATORY
PORT HUENEME, CALIFORNIA 93043-5003

OFFICIAL BUSINESS
PENALTY FOR PRIVATE USE, $300
1 IND-NCEL-2700/4 (REV. 12-73)
0930-LL-L70-0044

POSTAGE AND FEES PAID
DEPARTMENT OF THE NAVY
DOD-316

Commanding Officer
Code L14
Naval Civil Engineering Laboratory
Port Hueneme, California 93043-5003

DEPARTMENT OF THE NAVY

NAVAL CIVIL ENGINEERING LABORATORY
PORT HUENEME, CALIFORNIA 93043